Politecnico di Torino

Master thesis in mechanical engineering

Design of suction filter aimed to noise reduction of reciprocating piston compressor

Supervisors:

Prof. Eng.	Carlo	ROSSO
Eng.	Marco	ESPOSITO
Eng.	Maarten	VAN ACKER
Eng.	Margherita	BIUNDO

Candidate:

Francesco ALOSCHI

July 2019

INDEX

List of figures

List of tables

List of equation

ACKNOWLEDGEMENTS

Abstract

Air Piston compressor is a reciprocating machine that uses crack shaft mechanism to compress air. Usually this type of machine is quite noisy, typical noisy level are around 95 dB.This project is meant to look for noise sources and study a strategy to reduce the sound emitted. Thesis work was developed thanks to technical support and resources of Atlas Copco group, company leader in air compressor technique. One of the last machines designed in Atlas is Pat due machine, it will be the subject studied thought this research. This paper is meant to study the fluid dynamic noise source at compressor inlet, a new inlet filter concept will be designed according to fluid dynamics laws and tested. Finally, this thesis works will develop a method to build new acoustic filter that can reduce the overall machine noise. The new filter concept will be designed according to physics laws that governs fluid that flows down a duct, in details new prototype will be a combination of two different acoustic filters models (band stop model and expansion chamber).

Introduction

Basic principle of piston compressor machine & possible noise sources

Air piston compressor machine works with the positive displacement principle to deliver high pressure air. There is a crack shaft mechanism that pushes a piston inside a cylinder and thanks to a reciprocating movement it compresses air. Thermodynamically this type of machine works in in four phase: suction phase (ideally isobaric line 1 2), compression phase (isentropic line),discharge phase (isobaric line 2-3) and pressure reduction phase (isentropic line 3-4).Moreover, for engineering point of view if needed to reach higher pressure two or more compression phases can be employed by adding an intercooler between the first and the second stage, this technique was employed in PAT due machine that is double stage compressor and allow it to compress air up to $11 bar$,figure two depicts the thermodynamic cycle of a double stage compressor machine. In addition, double stage compressor will have higher efficiency and high compression ratio thanks to reduced work needed in the second stage.
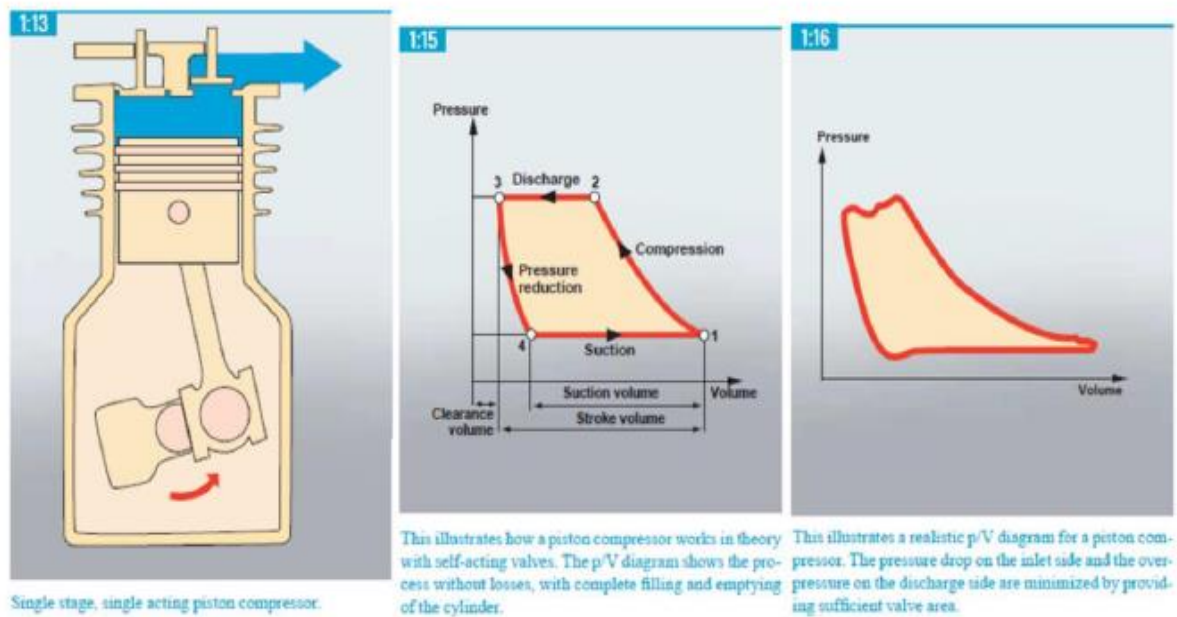
Figure 1- Working cycle of volumetric compressor [1]
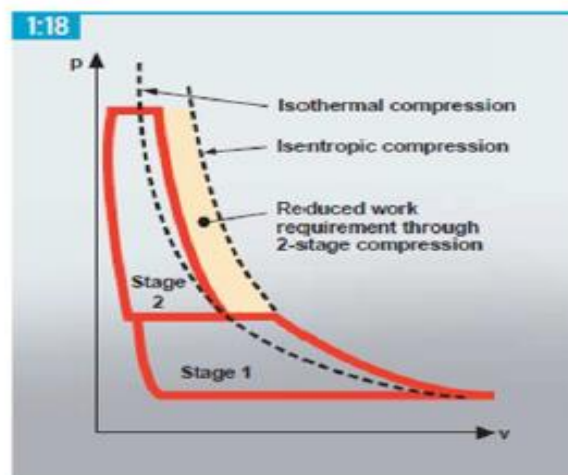
Figure 2- Double stage compressor cycle [1]

Nowadays, air piston compressor are quite noisy machines, typically the sound emitted by this type of machine is around $100dB$. One of the most challenging problems from engineering point of view is to understand the sources of sound and studying a strategy to reduce it. In addition, noise is one of the most important parameters that affects machine's price less therefore machine's noise is one of the main issues that a company have to afford in order to meet market requirement. In air piston compressor, noise comes from different sources such as air pulsation or mechanical vibrations, the aim of this thesis work is trying to understand how air pulsation affect the overall machine noise. Usually engineers employ proper designed dampers to reduce as much as possible mechanical vibrations noise

sources. Air filter can be meant as silencing devices that allow to reduce the machine's noise massively with relatively low-cost impact.

Chapter 1: Acoustic engineering basic definitions

1.1 Acoustic general information

Noise is generally defined as unwonted sound. In engineering field sound and noise are the same stuff both are related to waves propagations though a medium that can be solid, air or liquid (figure.3). Acoustic is branch of science that studied the propagations of sound thought a medium, as examples when a thin bar moves particles that surround it start to move and propagates in waves throughout surrounded medium as depicted in figure.3. It's observed that wave motion in medium is guided by small pressure variation, that is function of time and space.
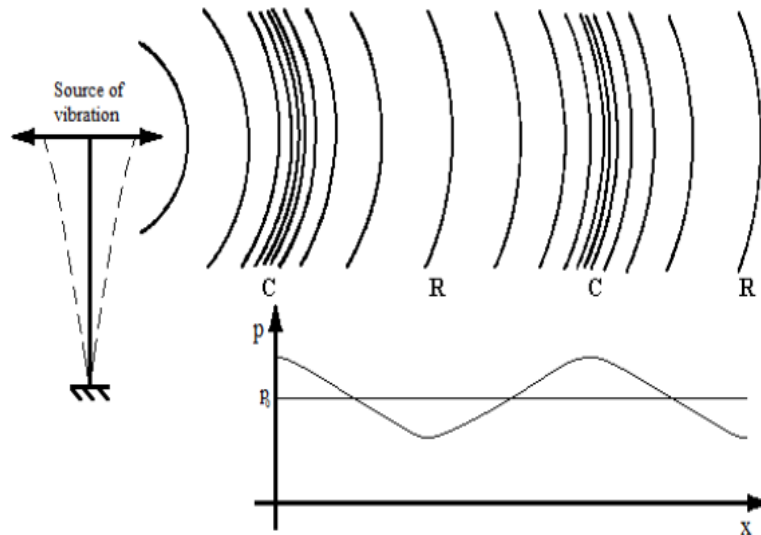
Figure 3- Propagation of sound waves in medium [1]

Sound is evaluated by three different quantities: sound pressure level, sound power level and sound intensity. Sound pressure level is measured with eq-1 where T is the wave period in [s], this quantity doesn't give any information about the source strength. For this reason, in engineering field is preferred to relate acoustic issues with sound power (eq.3) that is the amount of sound energy radiated per unit time. Sound power is defined thanks to the definition of sound intensity (eq.2) that is the product of sound pressure level and particles speed $\bar{v}$.

$$p_s[P_a] = \sqrt{1/T \int_0^T p_v(t)^2 dt}$$

Equation 1- Sound pressure level law

$$I_s[N/m^2 s] = p_s \bar{v}$$

Equation 2- Sound Intensity level

$$W_s[W] = \iint I_s dS$$

Equation 3- Sound power level

Moreover, acoustic quantities depicted above are ususally expressed in logartimic scale becaouse they vary in wide range . equations 4, 5, 6 represent respectively sound presure level,sound power level sound itesity level , all of this three quantities are refered to standards quantities(p_0, W_0, I_0).All acosutic quantity are related to standardard one becouse they represent the limit of audible for human hearing. Figure(4) gives an idea of how the sound emitted affects human hearing and gives an idea of decibels unit of measure, in that figure are listed on the left side of the stair a series of noise's sources while on the right side is present the quantity in Pascal of the prersure waves emitted.

$$L_p[dB] = 20 log_{10}(p_s/p_0)$$

Equation 4- Sound pressure level

$$L_w[dB] = 10 log_{10}(W_s/W_0)$$

Equation 5- Sound power level

$$L_I[dB] = 10 log_{10}(I_s/I_0)$$

Equation 6- sound intensity level

Where:

- $p_0 = 20 \ \mu P_a$
- $W_0 = 10^{-12} W$
- $I_0 = 10^{-12} W/m^2$
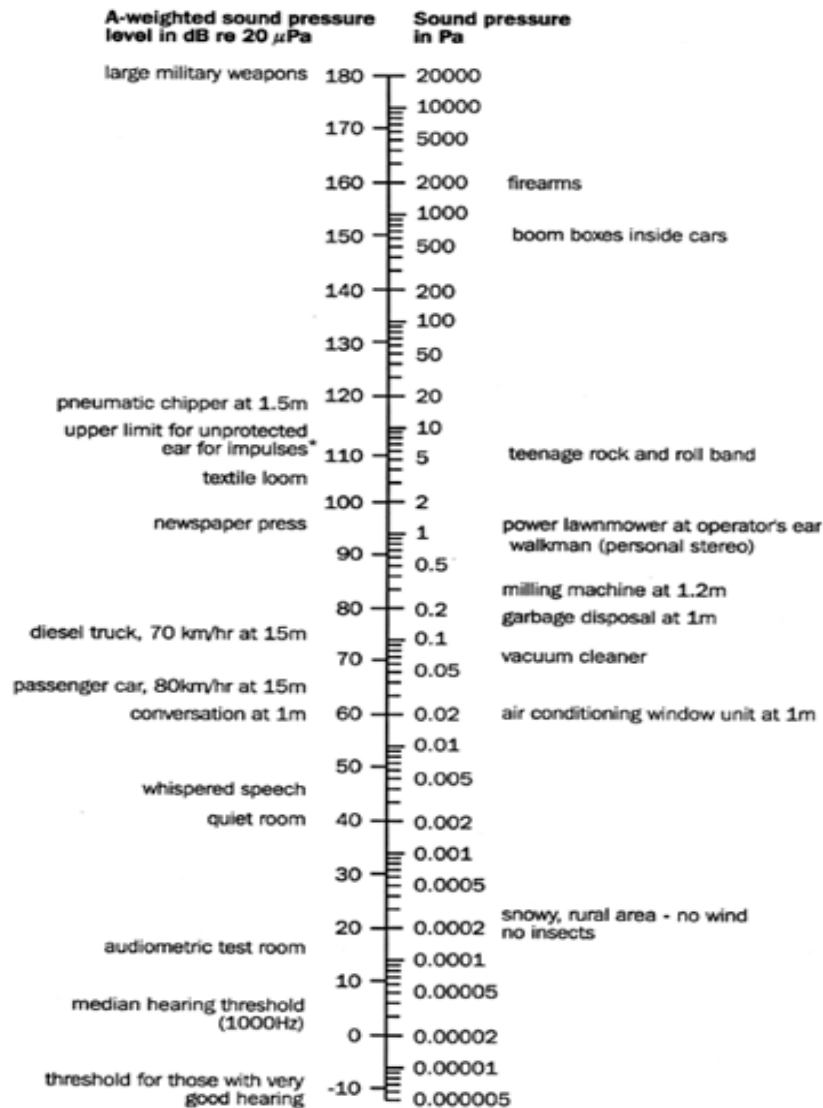
Figure 4- Decibels representation [2]

It's important to mentions that when a source generates an impulse the sound presure waves propagates with spheric front waves throught all directions in space, this consitions is called 'free field'. Sound waves propagates throght the medium in all directions without any obstacles that affects their reflection. This is the ideal condition that allow to estimate noise emitted by a source. In this project free field condition will be used to performe noise test. Noise level in free fiels strongly depend on the distance $r[m]$ from the noise source , it is easy to think that as more the reciver stay away from the source less is the sound intensisty percived. Figure 5 taken from the paper of professor profesor Colings H hanse [2] gives visual idea how the sound waves progates through medium while equation 7 highligh the effects of radius $r[m]$ on the sound presure level measurement.

$$L_p = L_w - 10log_{10}(4\pi r^2)$$

/Equation 7- sound pressure level in free field

13
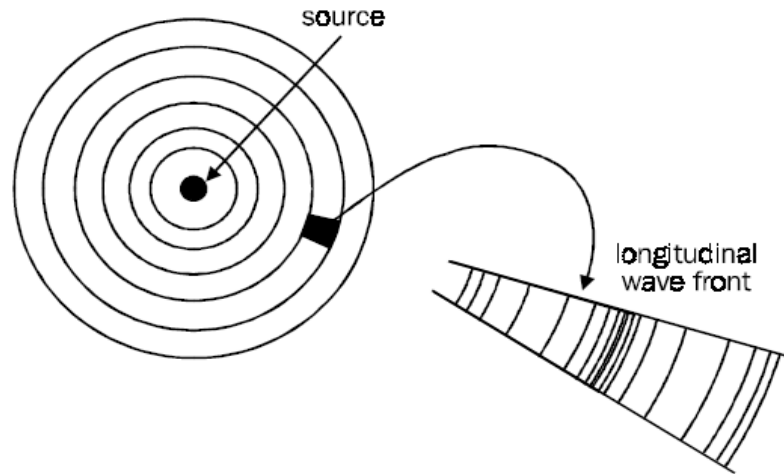
Figure 5-Representation of free field condition [2]

1.2 Sound spectrum frequency & noise measurment

In acoustic engineering, sound is studied in frequency domain, because it is important to know which frequency mainly affect sound emitted by machines. In addition, noise measurement is normalized according to $ISO\ 9614\ part\ 2$. All experimental results and measurement will be presented according to that norms and the overall sound power emitted will be expressed in $L_W(A)$ according to equation.7,terms A means that the overall sound power evaluated during the noise test is expressed in A-weighting scale. In development of noise measurement over the years different scales were built as shown in figure (6) below, each scale represented has different application according to the type of measure that have to be performed.
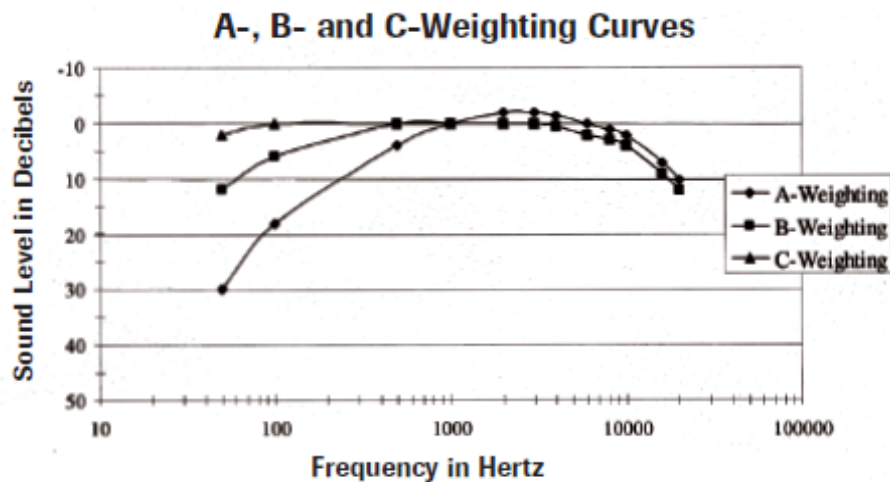
Figure 6-Representation of A,B,C ponderation curves [2]

A-weighted scale	It follows the sensitivity human's ears at low levels. It can predict well what risk human ear is affected. This scale filter mainly frequency in low frequency range and it is the most used in acoustic engineering and industrial application.
B-weighted scale	B scale follows the human sensitivity at moderate tone level. It was used to predict sound for loudspeaker application in the past
C-weighted scale	It follows the human sensitivity at high-frequency range, and it filter less frequency respect to A-scale and B-scale (flat spectrum frequency)

Table 1- Ponderation filter descriptions

$$L_w(A) = 10 * LOG(\sum_{n=1}^{n} 10^{Lw}/10)$$

Equation 8- A-weighted sound power level

Where:

- L_w sound power at a given frequency in $1/3$ of octave band
- $L_w(A)$ A − weighted sound power

When it's needed to analyse an acoustic sound source in frequency domain all frequencies will be dived equally in set of frequencies range called bands. Each band specify a specific range of frequency and a band is said to be octave when the upper band frequency is twice the lower. Usually in engineering application is used to group the whole frequency spectrum in one-third of octave band this allow to obtain

realisable results. One-third of octave band is narrower than octave band in this case the upper frequency is cube root of two times the lower frequency. Table.1 and table2 gives an example on how frequency range is split in frequencies band.

Lower- octave [Hz]	Centre-octave [Hz]	Upper- octave [Hz]
11	16	22
22	31.5	44
44	63	88
88	125	177
177	250	335
335	500	710
710	1000	1420
1420	2000	2840

Table 2- Octave band

Lower- 1/3 octave [Hz]	Centre-1/3 octave [Hz]	Upper 1/3 octave [Hz]
70.8	80	89.1
89.1	100	112
112	125	141
141	160	178
178	200	224
224	250	282
282	315	355
355	500	562

Table 3 - one third of octave band

Understanding machine's frequency spectrum is fundamental in acoustic engineering because it tells at which frequency a single component works and what contribution it gives on the overall noise emitted. This method is powerful, because it is possible affects the entire noise emitted by changing a single component design.

1.3 Noise test measurement set up

All experimental results that will be presented in this project will follow the ISO standard 9614 part two. This normative standardize the noise measurement of sound emitted by industrial machine and gives all indication and procedures for acquisition of acoustic data both in sound power and intensity pressure. It's important to recall that all noise's measurement effectuated in Pat due machine are taken with the pump running at maximum motor speed (1300 rpm) and when it releases the maximum pressure ($13 bar$), those are the heaviest conditions for Pat due machine. All experimental data reported in this project were taken in the same and with the same environment condition.

1.3.1 Measuring instrument

In order to perform acoustic test, a certified acoustic analyser will be employed figure.2 depict the Apollo analyser employed to detect acoustic waves emitted by machine, this analyser can also perform vibrations measurements. Apollo analyser is connected via cables with the acoustic probe figure (7) and computer that will post process all data collected. Acoustic probe is able to detect and measure sound pressure intensity in time domain. Analyzer automatically performs fast furrier transformation in order to pass the signal in time domain to frequency one. Output signal that gives the sound power spectrum of the noise test will be automatically filtered with low-pass filter that cut all the low-frequency that disturb the signal.

Figure 7- Apollo analyser

Figure 8-Sound probe instrument

1.3.2 Experiment set up

ISO standard 9614-part two uses scanning method over the enclosed surface to detect sound emitted by the machine. Indeed, sampling of measurement surface is reached by swept the enclosed surface area, as the surface is being painted. The following step were followed during the measurement season:

1. Calculate the external temperature, pressure and wind direction of surrounding environment, sound test has to be effectuated at standard condition ($T = 20°C \; and \; p[bar] = 1$
2. Definition of the noise source: this this are the maximum dimensions of PAT due pump
3. Definition of parallelepiped box that enclose the source. It is calculated by adding one meter to all dimension of the source. Table4 gives the dimensions of noise source and the enclosure box that were used for the experimental results. While table.5 reports the dimensions of the area that is detected by the probe. Figure.9 shows two box the grey's one represents the noise's source while the one built with yellow lines is the parallelepiped where the scanning probe takes the sound measurements. Figure.10 reports a pic of the experimental set-up, blue pales represent the acoustic surface area external to the source where the probe scan the acoustic waves emitted by machine.
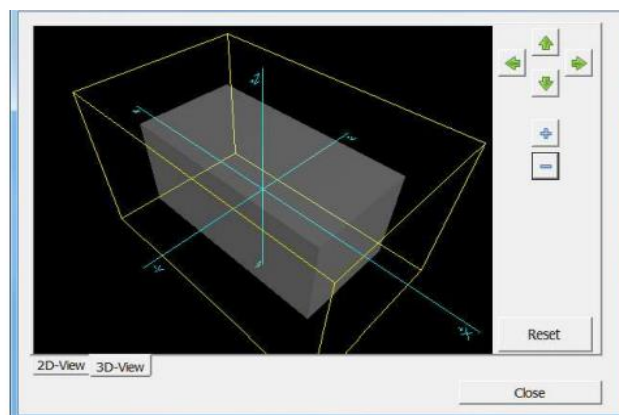
Figure 9- Enclosed box representation

Figure 10- PAT due experimental set up

Dimension	Length [m]	Width [m]	Height [m]
Source noise: pump	1.35	0.4	1.5
Source external box	2.35	1.4	2.5
Source offset	0	0	0

Table 4- Acoustic surface dimensions

Average measuring distance [m]	0.5
Effective surface area [m^2]	15

Table 5- Acoustic surface details dimensions

4. Scan the enclosed surfaces by swept the probe against it. Each face is scanned two times firstly with vertical movement and second with horizontal one. This procedure allows to reach engineering grade two level that is the limit of acceptability for engineering application. Table.6 shows the accuracy grade of this method it's worth to notice that A-weighted sound power will be affected by an error of 4 dB in overall. Scanning maybe done either manually or mechanically, if the operation is done manually it has to have a speed constant between 0.5 m/s to 1 m/s and the operation for a single surface scanned cannot be less than 20 seconds.
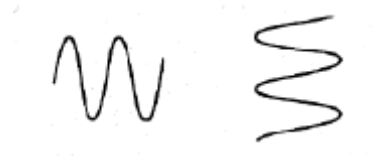
Figure 11- Scanning path method

One-third octave band centre frequencies [Hz]	Standard deviation (S*) in dB engineering (grade 2)	Survey (S*) in dB engineering (grade2)
50 -160	3	
200 - 630	2	
800 - 5000	1.5	
6300	2.5	
A weighted (50 Hz-6.3Hz)		4

Table 6 - Tolerance's definition in acoustic measurement

5. Scanning method gives a single value of spatial average sound intensity for each surface scanned then the software multiplies this value for the surface area and compute the value of sound power for each surface at different frequencies.

Chapter 2: Silent PAT due project

2.1 Thesis project general information

The aim of this thesis project is to improve the acoustic performance of PAT due pump (figure 12). As mentioned before air pulsation that flows through the pump significantly affect the overall machine noise. This project is meant to study their acoustic effect, one of the components that mainly control air flow inside the machine is the inlet filter, this will be the subject studied though this paperwork.

Figure 12- PAT due pump

All the measurements that will be reported in this paperwork were realized in free filed condition, using sound power intensity measuring device that will give the detailed machine's sound spectrum frequency response.

2.2 Pat due: Inlet Filter

Inlet filter (figure 14) is a simple device that if properly designed affects positively the overall machine's noise. Generally, an inlet filter is a cheap device typically made in plastic material that allow environment air to flow inside the pump. It creates a small depression between the environment and the pump, this affects machine's performance in terms of power absorbed and free air delivery. Free air delivery ($FAD[m^3/min]$) is the amount of flow that it is possible to extract from the compressor in ambient condition. Figure 13 shows pressure volume cycle that Pat due machine follows during working stage it is possible to evaluates maximum volume (V_{max}) and V_1 difference between them represent swept volume entrapped by compressor in the first compression stage. Equation 9 describes a way to compute theoretically FAD parameter (equation 10) this will help to calculate p_1 (effective inlet pressure of compression stage). Free air delivery is mainly controlled by run speed of compressor machine as more machine run at higher rotational speed more it delivers air. From experimental data it is possible compute effective initial pressure of start of compression p_1 that will be lower than ambient pressure. Combining equation 9 and 10 with experimental data of table (7) it is possible to evaluates the pressure drop (equation 13) down due to machine acoustic component and the effects that it will have on free air delivery (FAD). In this case pressure drop between external environment and first compression stage is 0.25bar this bring to effective loss of 25% of free air delivery.

21

$$n * \frac{p_a * V_a}{T_a} = n * \frac{p_1 * (V_{max} - V_1)}{T_1}$$

Equation 9- Equilibrium equation at filter inlet

$$FAD \ [l/min] = n * V_a$$

Equation 10 - FAD definition

$$dp \ [bar] \ = p_a - p_1$$

Equation 11- Pressure drop at inlet

Where:

- $n[rpm]$ *is the compressor running speed in cycle per minute*
- p_a *is the ambient presure* $1bar$ *or* $1.001Pa$
- V_a is the air volume delivered by compressor normalized in standard condition
- T_a *ambient temperature in stadard condition* $293 \ K$
- p_1 $[bar]$ *effective inlet presure where the compressor starts to compress air*
- $V_{max}[m^3]$*maximum entrapped volume capacity of PAT due machine*
- $V_1[m^3]$ *effective volume of start of compression*
- T_1 *effective temperature of compression stage start*

	No filter	PAT due filter
FAD [l/min]	581	436
Efficiency		75%
Pressure drop dp[bar]	0	0.21

Table 7 : PAT due filter actual design

Machine parameters	
$V_{max}[m\textasciicircum3]$	433*10^-6
$V_1[m\textasciicircum3]$	7.8*10^-6
$T_a[K]$	293
$T_1[K]$	293
$p_a[bar]$	1
$p_1[bar]$	0.78

Table 8 PAT due parameters
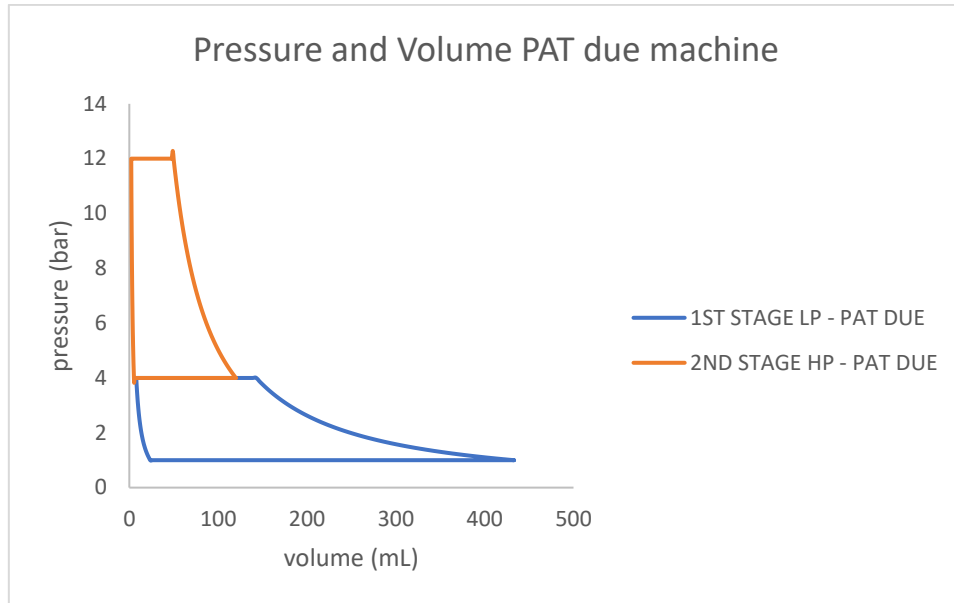
Figure 13-Experimental data of compression stage PAT due machine

Moreover, an absorption material element (that can be done in paper or polyester like in case of PAT due filter) has also the function to not allow dust or impurity to flow inside the compression chamber (figure 14). In the first stage design depression between ambient and inlet filter won't be considered but only the acoustic effects will be considered.
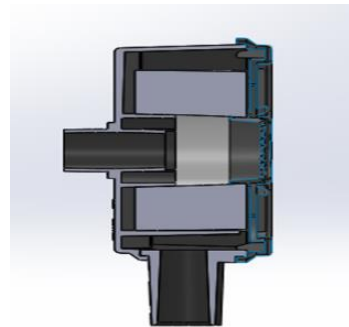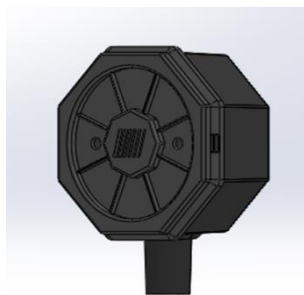
Figure 14-PAT due filter 3D representation

2.3 Acoustic's filter performance

In order to understand how many decibels, the actual filter improves the overall noise emitted and at which frequency ranges it works, two different noise tests according to ISO 9614 were performed (figure 15).
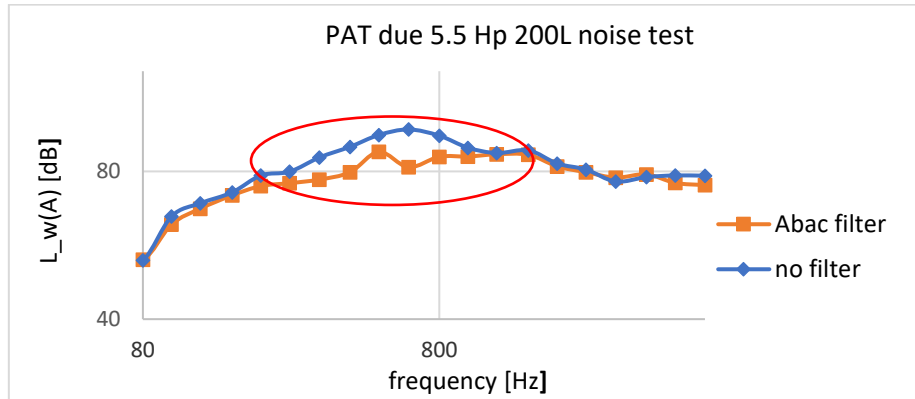
Figure 15-PAT due acoustic performance

From figure.15 it's evident that actual filter works mainly in low frequency range and it gives the main contribution at a frequency band near 630 Hz, it's worth to highlight the band frequency zone where it mainly works. Tabble.9 shows that this device reduces the overall sound emitted by 7.5 dB . it's clear that this acoustic element plays an important role at Low frequency range and massively affects the $L_w(A)$ of this pump.

Noise test PAT due 5.5Hp 200L	No filter	Pat due filter
Sound Power emitted $L_w(A)[dB]$	101.5	94
Difference respect to no filter [dB]		-7.5

Table 9- PAT due acosutic performance

Chapter 3: Filter design

New filter's concept will be created, and two different model will be developed in order to design properly the new silencing device. Figure.16 shows the logical

process that will be followed to achieve the goal. Firstly, general inlet filters behaviours will be investigated, and an analytical model will be implemented then a cad model of the concept will be built and simulated thanks to Ansys software simulator, this will help. Finally, new filter will be tested, and experimental result will be compared with the analytical and numerical ones. This method will be used two times, firstly to validate the actual PAT due filter and second to validate the new concept model.
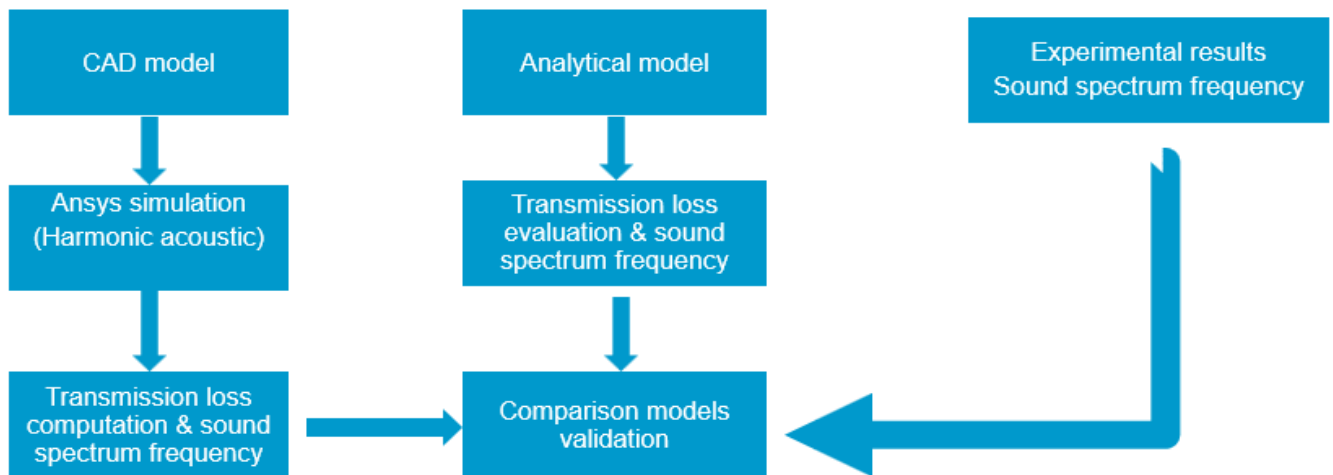
Figure 16 – Acoustic filter design process

3.1 Muffler and silencer general information

Muffler and silencer are devices used in different engineering application that can reduce sound emitted by machines, those devises work thanks to principle of waves that propagates down a duct. Silencing devices are classified in two different type:

- Absorptive or dissipative silencer uses absorption material inside (example: automotive muffler). Typically, those devises are employed in exhaust system for internal combustion engine
- Reactive silencer instead reflects back pressure wave thanks to geometry changes. Pressure wave energy is dissipated when fluid flows inside this device.

In our case inlet filter for piston compressor is classified as reactive silencer this means that shape affects sound attenuation behaviour.

3.2 Wave propagation in duct

Many acoustic problems involve conduction of sound down a duct, air. When a pressure wave flows inside a duct even if are present bends or obstacles it flows

down it. Equation.12 guides these physical phenomena , it is also called wave equation:

$$\frac{\partial^2 p(x,t)}{\partial pt^2} - c * \frac{\partial^2 p(x,t)}{\partial x^2} = p(t)$$

Equation 12- Wave equation

Where:

- $p[P_a] = pressure$
- $x[m] = coordinate\ space\ of\ duct$
- $t[s] = time$
- $c[m/s] = 343\ speed\ of\ sound$

Mathematical solution of equation.12 is:

$$p(x,t) = \left[A * e^{(-jkx)} + B * e^{(-j*k*x)}\right] * e^{j\omega t}$$

Equation 13- Mathematical solution of waves equation

Where:

- A is complex magnitude of propagating wave $[Pa]$
- B is complex magnitude of reflected wave $[Pa]$
- k is the wave number $[m]$
- ω is angular frequency $[s^{-1}]$
- j is imaginary number

Moreover, taking into consideration the particles speed equation 15 and volume speed equation 16 can be rearranged in 14 that represent the wave equation in simple form.

$$\rho * \frac{\partial u}{\partial t} - \frac{\partial p}{\partial u} = 0$$

Equation 14- wave equation simple form

$$u(x,t) = \frac{1}{\rho c}\left[A * e^{(-jkx)} + B * e^{(-j*k*x)}\right] * e^{j\omega t}$$

Equation 15- Particle speed law

$$v(x,t) = \frac{S}{\rho c}\left[A * e^{(-jkx)} + B * e^{(-j*k*x)}\right] * e^{j\omega t}$$

Equation 16- Volume speed law

Where:

- $u[m * s^{-1}]\ particles\ speed$
- $\rho[Kg * m^{-3}]\ is\ the\ density\ of\ the\ fluid$
- $S[m^2]$ duct cross sectional area
- $v[m^3 * s^{-1}]\ volume\ speed$

Above equations allow to evaluate **Transmission Loss** parameter, it describes the decrease of wave's energy that flows down a duct. Generally, Transmission loss is defined also as the ratio between sound power that hit muffler and the one transmitted at the outlet (equation 18).

$$\eta = \frac{v_{in} - v_{out}}{v_{in}}$$

Equation 17- Transmission loss coefficient

$$TL[dB] = 20 * log_{10}(\eta) = 20 * log_{10}\left|W_{in}\big/W_{out}\right|$$

Equation 18- Transmission loss formula

Where:

- $\eta[\ \ ]\ is\ the\ ratio\ between\ flow\ speed$
- $TL[dB]\ means\ Transmission\ Loss$
- $W_{in}\ sound\ power\ induced\ inside\ the\ duct$
- $W_{out}\ sound\ transmitted\ outside\ duct$
- "in" and "out" are for inlet and outlet duct cross section

3.3 Filter classification & performance parameters

Inlet Air filter are devises that can reduce noise propagation inside duct, they are meant as reactive silencer, so their geometry plays an in important role on performances. An acoustic filter works in specific frequency range they are classified in: high pass, low pass and band-stop filter. All these filter's model will be analysed thank to the help of the studies conducted by Daniel A.Russel in is research of acoustic filter and will be presented in detail below[3].

3.3.1 Low pass filter

A simple scheme of high pass filter is showed in figure.17, it is a simple duct where an expansion chamber is added. This filter's type allows low- frequency band to pass while can attenuate high frequency -bands. Transmission loss equation can be

founded in literature and for simple filter with same diameter at input and outlet is evaluated with equation 19. This model is function of shape geometry of the filter and the wave number (equation 20).
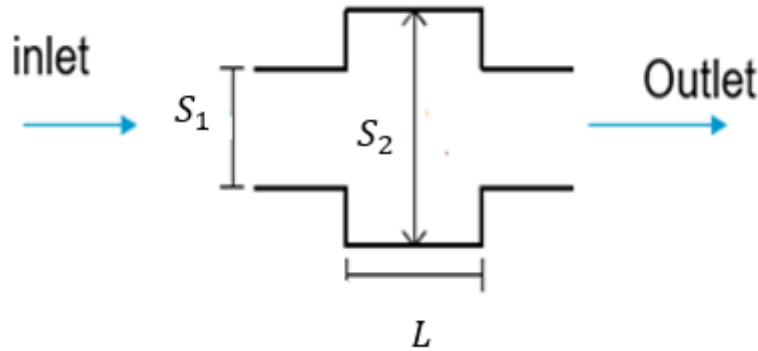
Figure 17-Law pass filter

$$TL[dB] = 20 * \log_{10}\left[1/4 * \left(4 * \cos^2(\text{kL}) + (m + 1/m)^2 * \sin^2(k * \text{L})\right)\right]$$

Equation 19- Transmission loss of low pass filter

$$k = f/c$$

Equation 20- Wave number

Where:

- $S_1 = D_1^2 * \pi/4$ equation of the imput filter's surface and D_1 is inlet diameter
- $S_2 = D_2^2 * \pi/4$ equation of the expantion chamber surface D_2 is expantion chamber diameter
- $m[\ \ ]$ ratio between (S_1/S_2)
- $L[m]$ length of expantion chamber
- k is the wave number
- f is frequency in $[Hz]$
- c is the speed of sound $[m/s]$

3.3.2 High pass filter

High pass filter look like tube pipe where is inserted a "T" junction with an open hole figure.18. It works in high frequency range while pass low-frequancy ones, Transmission Loss for this filter's type is evaluated with equation 21.
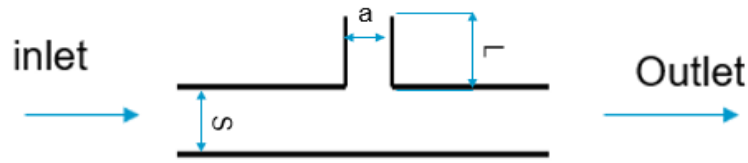
Figure 18- High pass filter

$$TL[dB] = 20 * log_{10}\left(1 + \left[\frac{\pi * a^2 * f}{2 * S * (L + 1.5 * a)}\right]\right)^{-1}$$

Equation 21- Transmission loss high pass filter

Where:

- $a[mm]$ is the diameter of the "T" juction
- $L[mm]$ is the lenght of "T" junction

3.3.3 Band stop model (Helmholtz resonator)

Band stop filter or Helmholtz resonator is a closed chamber inserted in the main tube pipe that creates a resonant frequency (f_r $resonat$ $frequency$) that absorb the acoustic energy at that frequency . Geometrical parameters that are shown in figigure19 gives the resonant frequency where this device works. In addition is possible to represent it like mass-spring system model (Figure.19).
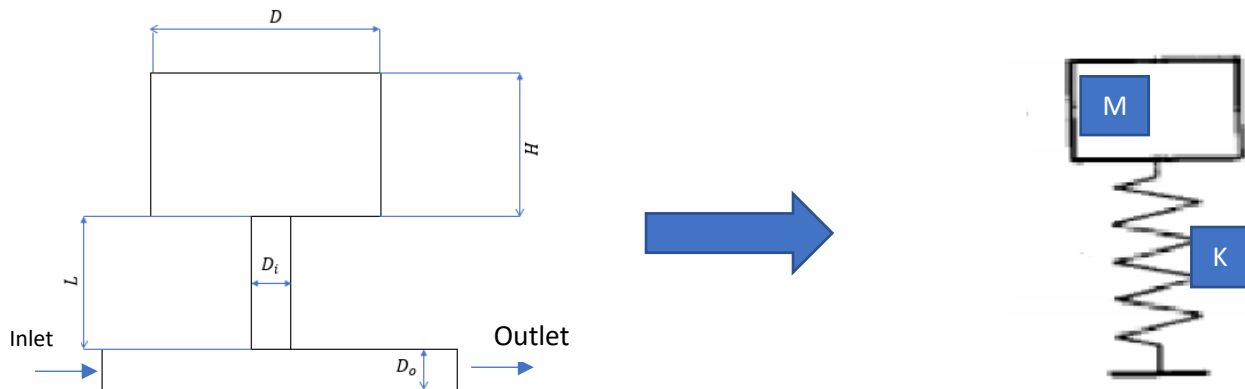
Figure 19- Mass-spring model on the right and band-stop model on the left

Starting from the classic mathematical model of a mass-spring system (eq.22) it is possible to derive resonant frequency of the system (eq.23) and the connection with the acoustic field. Introducing air density and geometry parameter of band-stop model it is possible to evaluate its resonant frequency (eq.24) by combining equation.(22 and 23) . Finally, Transmission Loss parameter is given considering the previous theory of fluid inside duct by equation (27).

$$m\ddot{X} + K\dot{X} = 0$$

Equation 22- Dynamic equation

$$f_r[Hz] = \frac{1}{2*\pi}\sqrt{\frac{K}{m}}$$

Equation 23 - Resonant frequency

$$m = \rho * S_i * L$$

Equation 24 - Mass definition

$$K = \rho c^2 * \frac{S^2}{V}$$

Equation 25 - Stiffness definition

$$f_r[Hz] = \frac{c}{2*\pi} * \sqrt{\frac{S_i}{V*L}}$$

Equation 26- Resonant frequency in band stop model

$$TL[dB] = 20 * log_{10}\left(1 + \left[\left(\sqrt{\frac{V*S_i}{L}}/2*S_o\right)/(f/f_r - f_r/f)\right]\right)$$

Equation 27- Transmission loss law for band stop model

Where:

- ρ air $dencity$ at $20°\,C$
- $m[Kg]$ $mass$ of the $model$
- $K\,[Nm]$ $stiffness$ of the $system$
- c $sound$ $speed$
- L, H, D_i, D_o, D $geoemtric$ $paramenters$ in $[mm]$ of $band-stop$ $model$
- $V[mm^3] = \pi * H * D^2/4$ $entrapped$ $chamber$ $volume$
- $S_i[mm^2] = \pi * d_i^2/4 surface$ $area$ of $inlet$ $tube$ $chamber$
- $S_o[mm^2] = \pi * d_o^2/4 surface$ $area$ of the $main$ $pipe$

3.4 Finite element method: Ansys simulator

Ansys software is a finite element simulator that thanks to his "Harmonic acoustic" module allow to compute the Transmission Loss of a silencing device; this will help

to optimize the analytical model of new filter concept, giving detailed results. In this paper two different simulation will be presented one is for the actual filter element an and second for the new one concept, both results will be compared with analytical model and experimental one.

3.4.1 Harmonic acoustic steps

Harmonic acoustic Ansys's is created to implement waves equation described in chapter 3.1 by taking in input the geometry of the acoustic component and using the transmittance matrix method it generates the transmission loss characteristic of the acoustic component. In order to perform this simulation, the following steps are depicted:

- Cad geometry and material definition: figure.20 shows cad geometry imported; it is fundamental that it will be a single solid unit because defines also the acoustic environment that will be associated to the medium where acoustic waves propagate. In our case the medium is the air, table.10 depicts material property for that simulation.
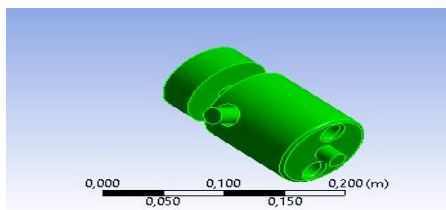
Figure 20 – CAD geometry definition

Air Property	
Density $[Kg/m^3]$	1.2250
Thermal conductivity $[W/m°C]$	0.02420
Specific heat $[J/Kg°C]$	1006.4
Sound speed in medium $[m/s]$	343

Table 10 - Air property definition

- Mesh: next step after geometry and acoustic space preparation is meshing (figure 22). In this case FLUID221 elements type will be used, FLUID211 is a 10-node element (figure 21) that is employed in Ansys to simulate fluid medium in our case air that flows inside filter.
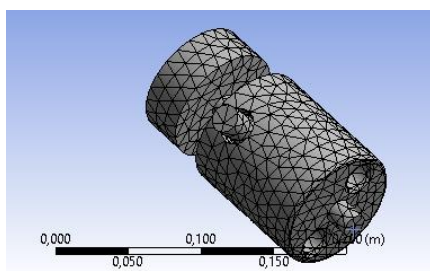
Figure 22- Mesh details
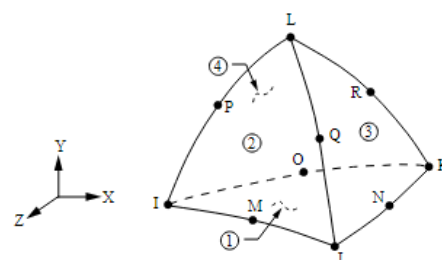
Figure 21- Finite element fluid 221

- Next, Harmonic acoustic module requires to set different parameters:
  1. **Acoustic region** that simulate the air volume entrapped by geometry (figure 23)
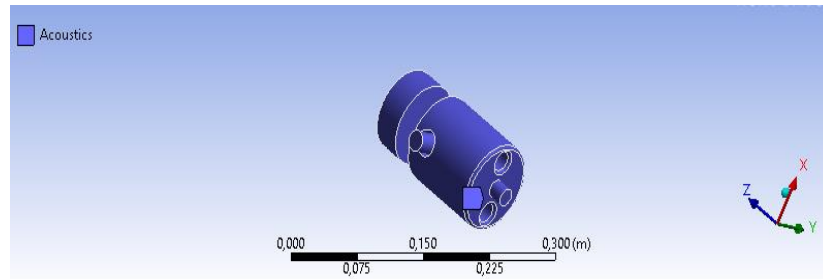
Figure 23 - Acoustic domain

  2. **Surface velocity** is the initial fluid speed that hit input port, it simulates input vibration that causes waves flow dawn the filter (figure 24),for our simulation input speed can be assumed to be $-0.001m/s$ that is a value close $0m/s$.
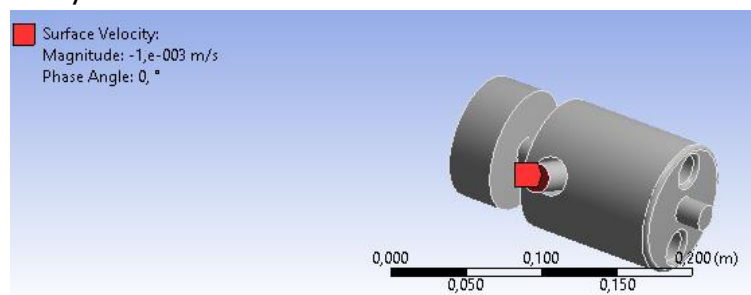
Figure 24 – Surface speed

  3. **Radiation boundary** that are two surfaces where there isn't waves reflection (figure.25) so only transmitted waves will be considered for transmission loss computation
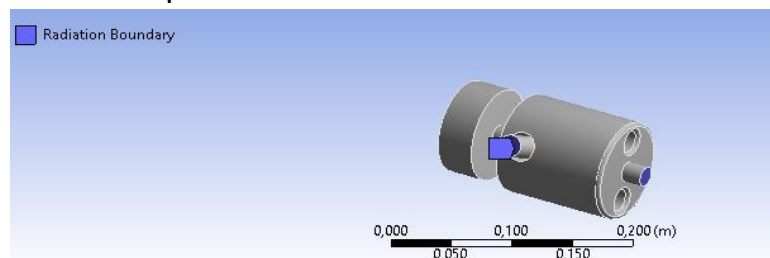
Figure 25 - Radiation boundary

  4. **Inlet and outlet port surfaces** those two surfaces (figure 26) represent the acoustic region where the transmission loss is evaluated, it computes sound power transmitted between two port by considering geometry changes through the component.
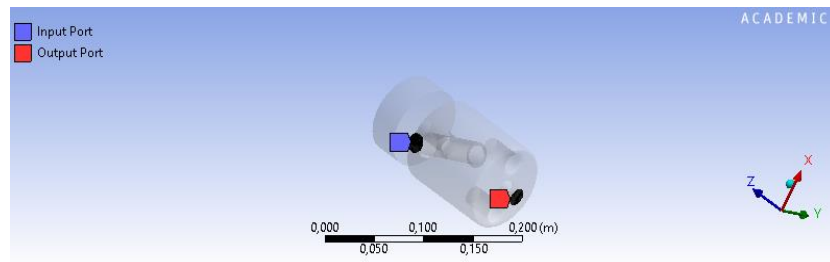
Figure 26 - Input and output port

- Finally, Ansys requires to set the frequency band wanted in our case same frequencies band that are measured by the acoustic analyser (1/3 of octave) will be employed.

3.5 Validation of actual Pat due acoustic filter

The beginning stage of the design was the classification of the actual model of PAT due filter in one of the filter's type depicted in the previous sections (Low-pass, high-pass or band-band stop). Experimentally, it is possible extract the Transmission Loss curve (figure.27), this curve is computed by making the difference frequency per frequency of the sound power spectrum frequency with and without filter element .From transmission loss curve (figure.27) is evident that this filter works mainly in frequency range near 630 Hz, so for this reason it is treated as band-stop model where the resonant frequency corresponds to the pick of the curve. Input parameters that describes the resonant frequency (f_r) and **transmission loss** of a band stop model ($equation\ 26\ and\ 27$) are reported in table11.It's evident that exist a strong dependence between filter shape and transmission loss curve and also that the simple analytical band-stop model depicts with small error the reality (see figure.29).
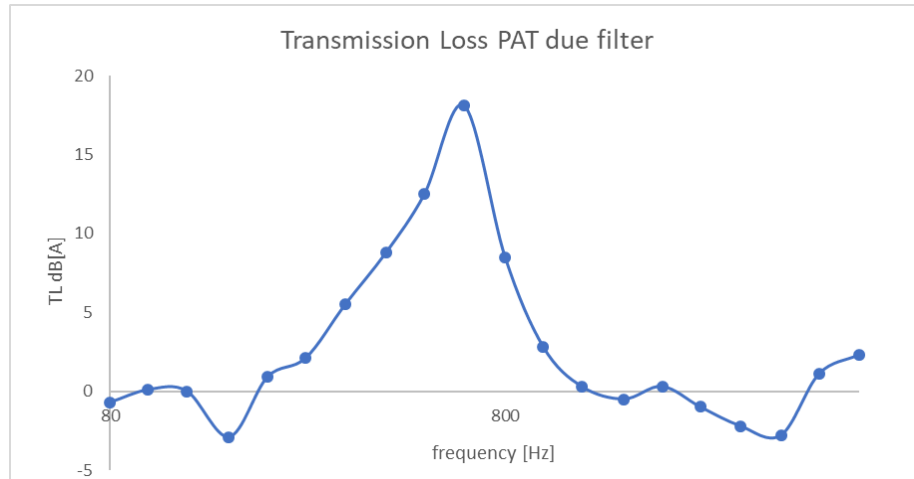
Figure 27 - Pat due filter transmission loss

Geometric parameters
PAT due filter

$D[mm]$	90
$H[mm]$	35
$D_i\,[mm]$	17.8
$D_o[mm]$	17.5
$L[mm]$	35
$c(speed\;of\;sound)[m/s]$	342

Table 11 – Pat due filter geometry parameters

In figure 28. is represented in detail how Pat due filter can be represented with band stop model. All shape will be simplified (example the octagonal shape present in front view will be assumed to be circular).
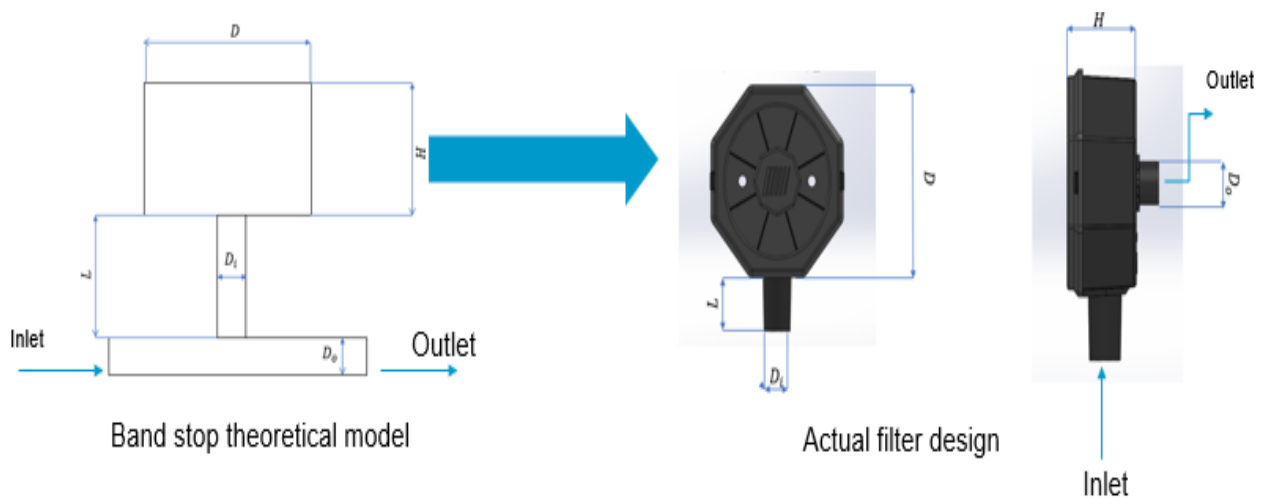
Figure 28: Pat due filter validation model
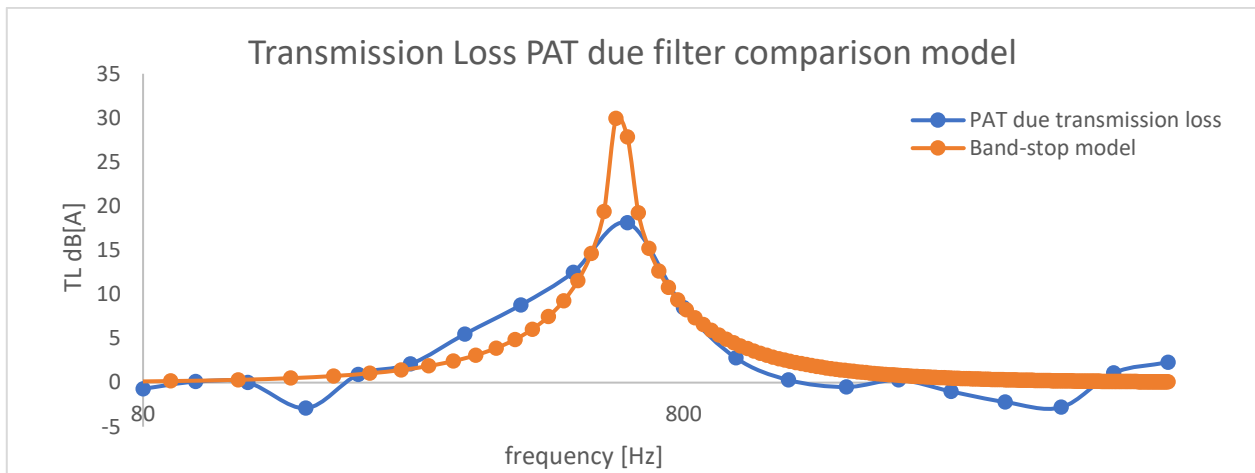
Figure 29 - Comparison model between Pat due filter and band-stop model

Moreover thanks to the Cad model provided by the company an acoustic simulation (Ansys software) is perfoemed and the sound power spectrum frequency curve will be comapared with the analytical model and experimental one (figure.30). Sound power spectrum curves were coputed by the difference frequency by frequency between Transmission loss of each model and sound spectrum frequency of no-filter test. e Numerical model is complex respect to the analysitcal one beacause it take into account all the possible geometry details. It's obesrved that numerical model relized has quite good accuracy in low-frequancy range while does not give good results in high frequency range.
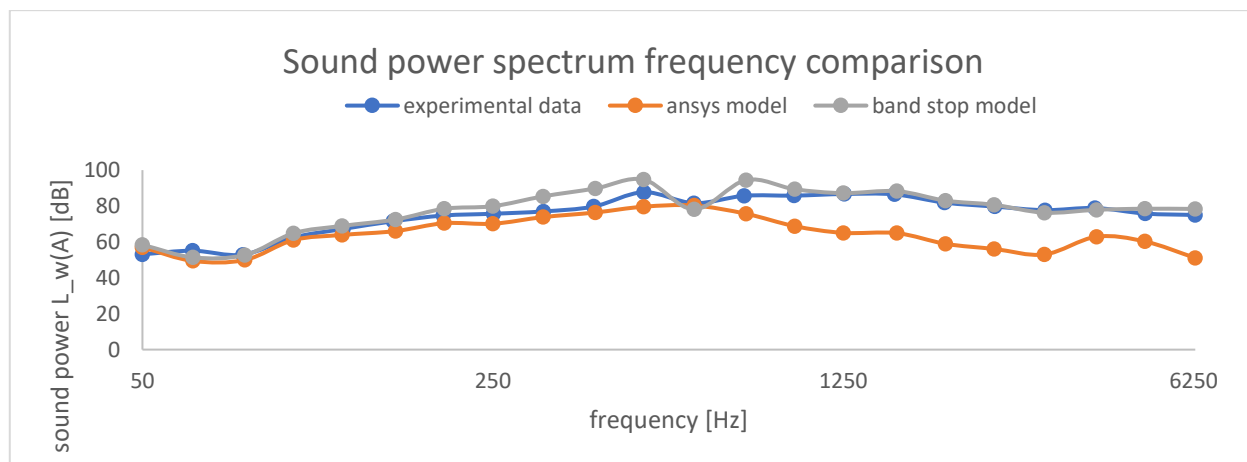
Figure 30 -Sound spectrum frequency models comparison

In addition, sensitivity analysis that compares all two model with experimental is show in table.12. Here below are reported all the errors between models it's evident that analytical model represents with quite good approximation the actual filter reality.

Model: Pat due filter	%error in $Lw(A)$ average	%error Max in Lw

Analytical- band stop model	5%	16%
Ansys model	13%	32%

Table 12 - sensitivity analysis

Finally, it is worth to observe that even is analytical model takes less inputs parameters and doesn't considers shapes different shapes that inside the filter in this case it's more reliable respect to Ansys model.

3.6 New filter CAD model

New design concept will be realized by taking into consideration all the previous theory on acoustic filters. In details new filter concept will be realized by merging the positive effects of expansion chamber and band -stop model. Scheme below shows the geometry details of new filter concept; it is composed by band stop model tuned at 630 Hz and expansion chamber that should be tune high frequency range figure.31. Figure (32 and 33) shows the transmission loss curves of expansion chamber and band stop currently employed in new filter concept design. Those curves follow equations 26 and 27 and as depicted in previous section those model strongly depend on the geometry parameter, inputs parameter for those models are present in tables 13 and 14.
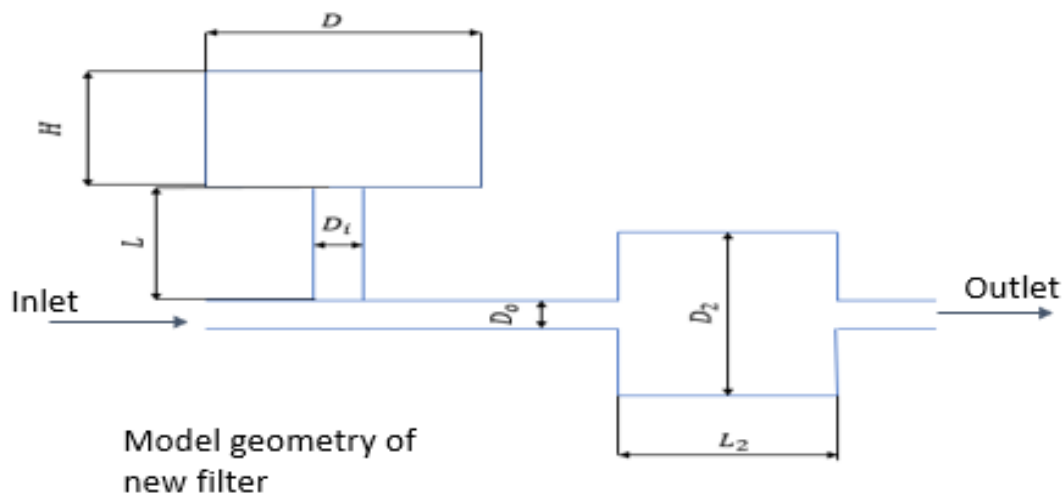
Figure 31 - scheme representation of new filter concept
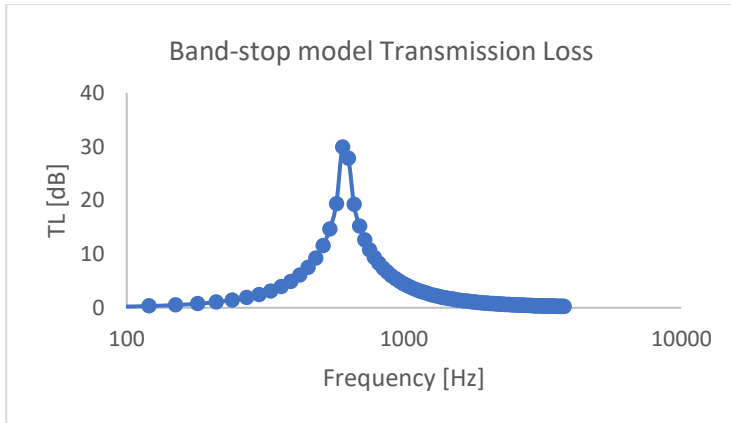
Figure 32 - Band- stop model curve of new filter concept

Geometric parameters band-stop model	
$D[mm]$	90
$H[mm]$	35
$D_i[mm]$	17.8
$D_o[mm]$	17.5
$L[mm]$	35
$c(sound's\ speed)[m/s]$	340

Table 13 - Geometry parameters of band stop
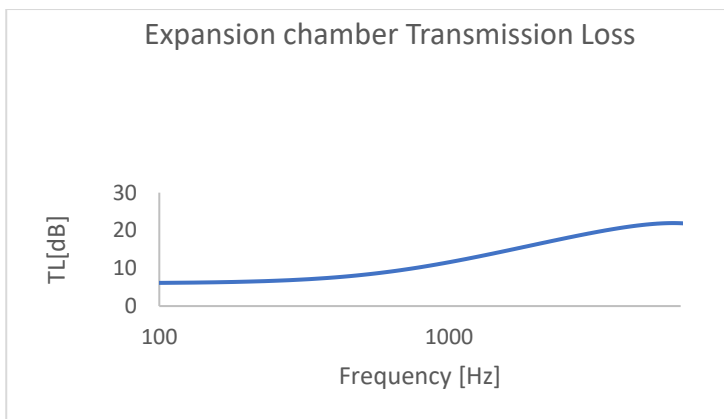
Figure 33- Expansion chamber model of new filter concept

Geometry parameters of expansion chamber	
$D_o[mm]$	17.5
$L_2[mm]$	90
$D_2[mm]$	90

Table 14 - Geometry parameters of expansion chamber model

In addition, inside the expansion chamber a honeycomb grid is inserted, this shape will help to improve transmission loss in medium frequency rage. Thanks to superposition principle it is possible to build an analytical model of new filter concept that considers all the geometry effects on transmission loss curve.

3.6.1 Honeycomb behaviour design

Tanks to the courtesy of *R. Galgalikar, "DESIGN AUTOMATION AND OPTIMIZATION OF HONEYCOMB STRUCTURES FOR MAXIMUM SOUND,"*[4] , it is possible to find an analytical method to evaluate the effects that honeycomb shape has in sound transmission loss, thanks to this geometry it's possible to decelerates the fluid that flow down the device and so consistently improve filter's acoustic behaviour.

Honeycomb grid shape is used to attenuate the sound and heat transfer in multiples engineering solution. Experimentally, figure.34 shows typical sound transmission loss curve of sheet panel, it is possible to define three regions: the first is correlated by the plate bending stiffness ,the second is controlled by the mass-law equation, finally the dip in third region is due to the resonance frequency of the plate. In our case it was possible to analytically model the filter's grid thanks to the mass-low even if only the mid-frequency range will be considered reliable [50Hz-1500Hz]. Equation (28) is mass law equation that describes the transmission loss behaviour of panel, it is function of the wave's frequency ($\omega[rad/s]$) and surface mass "m" that strongly depend on the material and honeycomb shape. Here below are reported all geometry details that affects honeycomb shape and so the transmission loss behaviour.

$$TL_{HC} = 20 * log_{10}[1 + (^{m\omega cos(\theta)}/_{2\rho c})]$$

Equation 28 - Honey comb transmission loss equation

Where:

- θ incidence waves angle that for sake of simplicity will be assumed 0°. It is the angle at which the acoustic waves hit the honeycomb grid surface
- ρ & c are the air density and air's speed of sound at 20° and 1[bar]
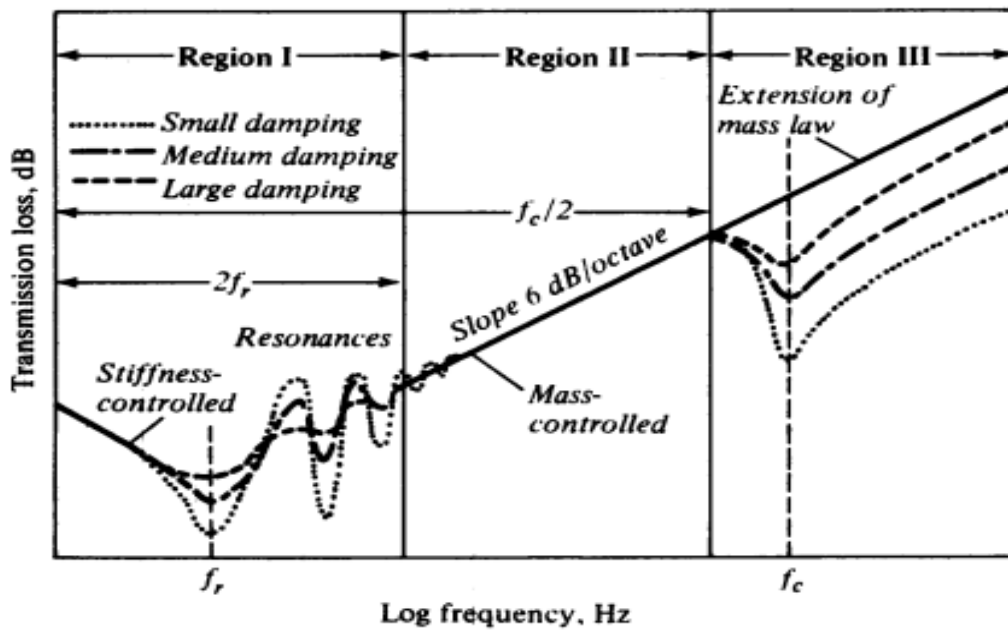- $m[Kg/m^2]$ is the mass per unit area of the honeycomb grid

Figure 34- Honey comb theoretical behaviour [5]

The dip in third region occurs at equation.29 where B represent the bending stiffness of the grid.

$$f_c = c^2/2\pi\sqrt{\rho_m/B}$$

Equation 29 - resonant frequency in third region

The most relevant quantity that is related to sound transmission loss of a honeycomb grid is mass per unit area m[Kg/m^2], this is function of the material of grid (in our PETG polymer) and core size geometry design. In order to proper characterize the mass per unit area of honeycomb grid the following steps were computed:

1. Evaluation of honeycomb density: it is computed by simply geometrical consideration that relates the geometry of the honeycomb core $(t, l, h, \varphi\ are\ the\ gometry\ dimension\ of\ core)$ and $\rho_h[Kg/m^3]$ that is the density of the honeycomb shape which is lower than ρ_m density of the material in our case PETG.

$$\rho_h[Kg/m^3] = \rho_m \frac{(t/l)(h/l + 2)}{2cos(\varphi)(h/l + sin(\varphi)}$$

Equation 30 - Density of honeycomb grid

Where:
- t, l, h are geometry parameter of honeycomb grid (figure.35) in [mm]
- φ [°] is the angle of hexagon geometry of honeycomb core
- ρ_h and ρ_m are respectively the effective density of honeycomb geometry and material density
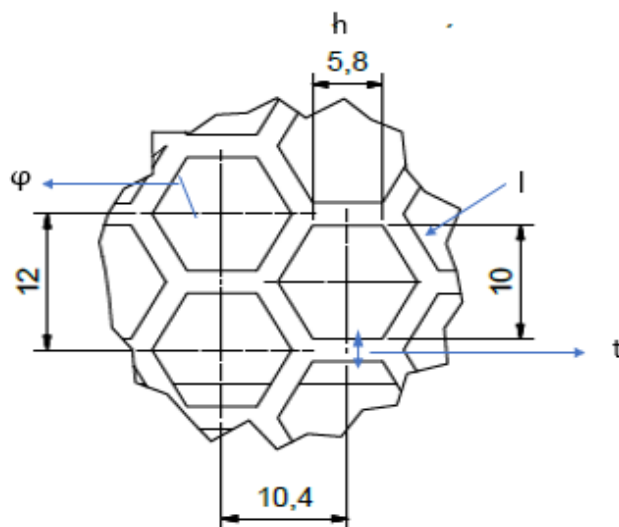

Figure 35- Honeycomb core details

2. Computation of honeycomb surface and volume equation(31 and 32) and mass $M_{grid}[Kg]$ equation(33)

$$V_h[m^3] = D_{grid}^{\;2} * \pi/4 * t_s$$

Equation 31- volume grid law

$$S_{grid}[m^2] = D_{grid}^{\;2} * \pi/4$$

Equation 32- Surface grid law

$$M_{grid}[Kg] = \rho_h * V_h$$

Equation 33- Mass grid law

Where:

- $D_{grid}\,[mm]$ and $t_s[mm]$ are grid's diameter and thickness

3. Finally, mass per unit surface ($m[Kg/m^2]$) is computed taking into consideration all previous parameter, it is the ratio between the honeycomb mass and surface.

$$m[Kg/m^2]=M_{grid}/S_{grid}$$

Equation 34- Mass per unit surface

Tables 16 and 17 bellow shows all geometry and material data useful to calculate the effect that honeycomb grid gave to transmission loss characteristic.

PETG material property

Density $\rho_m[Kg/m^3]$	$1.26 * 10^3$
Yield strength	4.79e7
Tensile strength	6.6e7
Elongation	1.18 %
Hardness	1.41e8
Young modulus	2.01e9

Table 15 - PETG material property

Honeycomb geometry parameter design

l[mm]	5.8
h[mm]	5.8
t[mm]	2

$\varphi[°]$	30
$M_{grid}[Kg]$	0.081
$V_h[mm^3]$	16344
$\rho_h[Kg/m^3]$	501.7
$M[Kg/m^2]$	10
$S_{grid}[mm^2]$	8167
$t_s[mm]$	12

Table 16 - Honey comb geometry parameters

Figure.36 below shows theoretical transmission loss behaviour of honeycomb shape that is inserted inside new filter, as mention before it can give reliable result only in mid frequency range since its effect at high frequency range can be affected by different phenomena not considered in that model. This curve follows mass-controlled region given by transmission loss equation.28. As shown from that graph honeycomb geometry affects in minor extent transmission loss respect to expansion chamber or band stop model but it will give a positive contribution to the overall sound emitted.
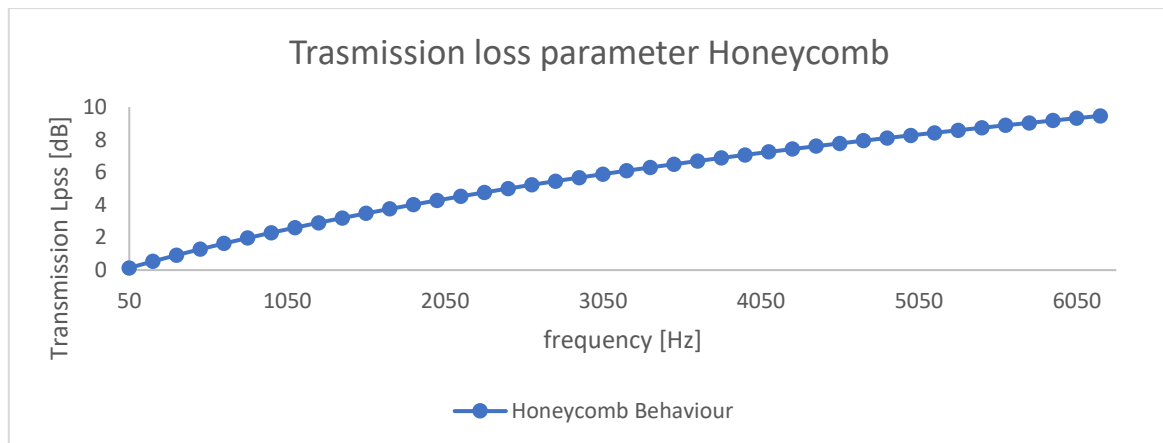

Figure 36 - Honeycomb effect

3.6.2 Superposition principle and analytical filter's model

New filter concept is modelled as linear system, so it satisfies the superposition theorem. This principle is widely employed in many engineering problems to depict complex linear system that has multiple inputs. In this case new filter model has to take into account three different effects that gives the input of the model. Superposition principle will give the transmission loss of our complex system that as mentioned before it's composed by three acoustic device models (expansion chamber, band-stop and honeycomb panel). Three transfer function represent each of model and those three have to be merged to find the final analytical model. Since all these three models are in frequency domain it is possible to sum up their effects

by multiplying their function frequency by frequency. Here bellow are reported three equation (equation.35,36,37) and the final equation.38 that represents the analytical model of the filter that is the product of the first three function. Figure.37 depicts the theoretical transmission loss of new filter concept, it is possible to observe the pick due to band stop resonator and also the linearity given by expansion chamber and honeycomb grid.

$$TL_{HC} = 20 * log_{10}[1 + (^{m\omega cos(\theta)}/_{2\rho c}]$$

Equation 35 - Honey comb transmission loss law

$$TL_{EX}[dB] = 20 * log_{10}\left[1/4 * \left(4 * cos^2(kL) + (m + 1/m)^2 * sin^2(k*L)\right)\right]$$

Equation 36- Expansion chamber law

$$TL_{BS}[dB] = 20 * log_{10}\left(1 + \left[\left(\sqrt{\frac{V*S_i}{L}}/2*S_o\right)/(f/f_r - f_r/f)\right]\right)$$

Equation 37-band stop model law

$$TL_{total} = TL_{BS} * TL_{EX} * TL_{HC}$$

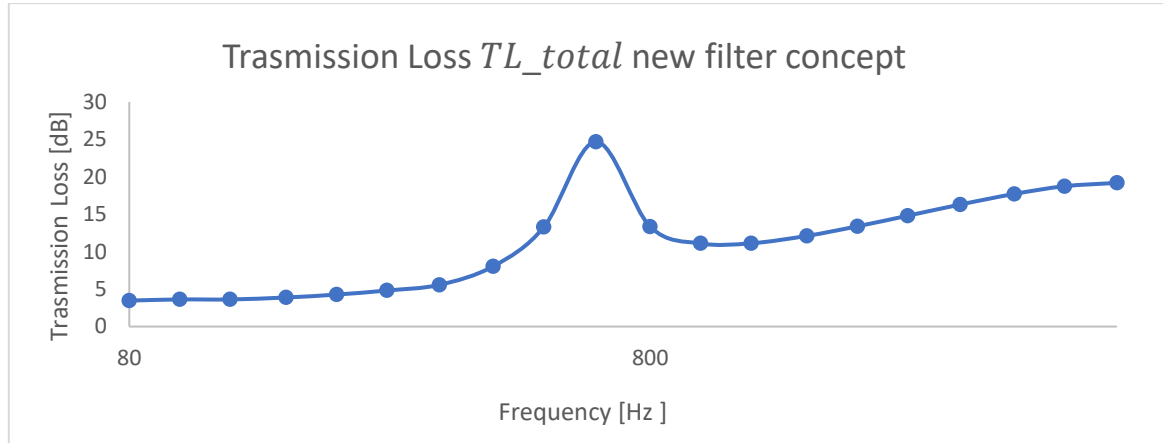*Equation 38- Superposition theorem*

Figure 37– Theoretical transmission loss curve of new filter concept

Finally, the above analytical model together with the Ansys one, allows to estimate theoretically total sound power emitted by PAT due pump. Here below is reported a table where a theoretical estimation of $L_w(A)$ is present. A-weighted sound power estimation is computed by subtracting transmission loss curve to sound power spectrum frequency of no filter noise machine test and applying equation.38, those results will be compared with experimental results.

3.7 3D CAD model of concept filter & assembly

Figure (38) shows 3D model of PAT due head, it is the pump's components where inlet filter compressor will be assembled with. In details the only design constrain that were afforded related the distance and size between two holes depicted in figure (11).
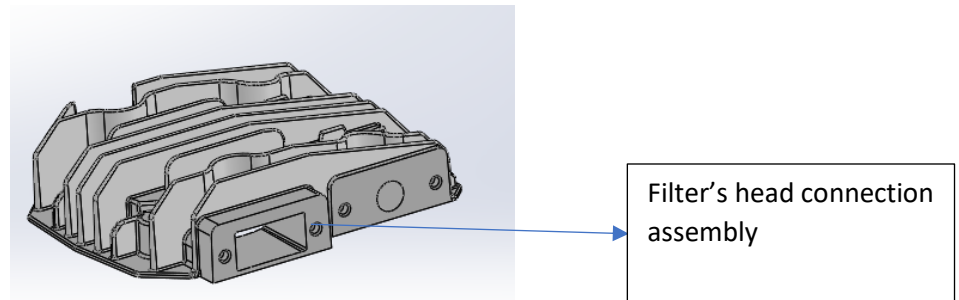

Filter's head connection assembly

Figure 38- 3D model PAT due filter's head

Figure.39 below shows the details of new filter cad assembly in details it is possible to observe the section view and isometric view. In section view it worth to observe that two M6 screws that connect acoustic device with head filter component where employed while four M4 screws where adopted to joins two filter's parts.
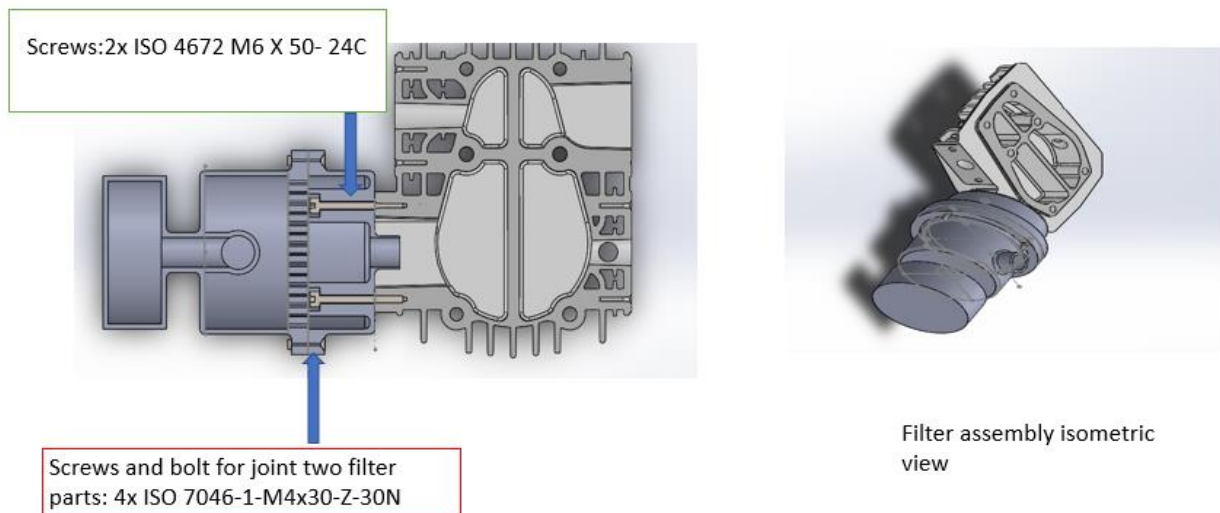

Screws:2x ISO 4672 M6 X 50- 24C

Screws and bolt for joint two filter parts: 4x ISO 7046-1-M4x30-Z-30N

Filter assembly isometric view

Figure 39- Air filter assembly.

As shown in filter assembly news design concept is realized in two different part. Figure.40 depicts the filter outlet where four hole (for M4 crews) that are realized in the external crown and other two holes inside the component where M6 screws are places for connection with filter's head. Moreover, inside this part is placed also the

foam sponge that has the only function to collect dust and other impurity that could flow inside the pump. Foam element wasn't evaluated as acoustic element in this thesis project even if in literature is was proven that air filter material can be affect in minor extent air filter performance.
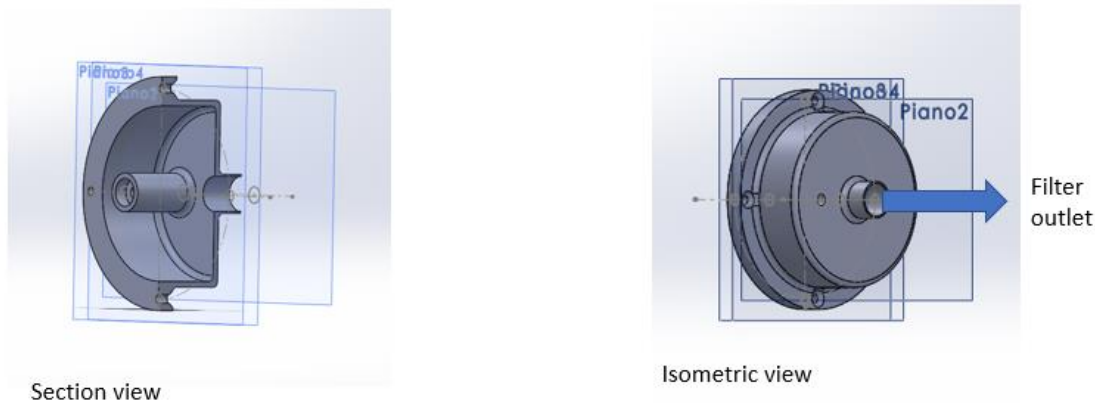

Figure 40- New filter's concept outlet

Figure 41 shows foam material assembly picture on left depicts 3D view of sponge material while on the right it is present the assembly with filter's head part. In the image on the right foam is represented by red part.
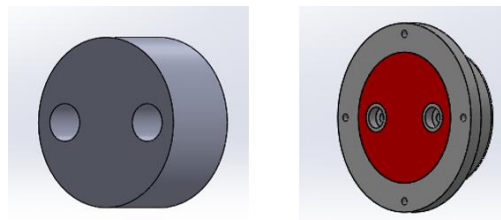

Figure 41- Foam material assembly

Finally, the third component of new concept design is the filter inlet, here are present both the band stop resonator and honeycomb grid. This is the most complex part of the new component also I this case there is the crown outside the expansion chamber where are present four holes that are connected in pairs with ones of filter's outlet.
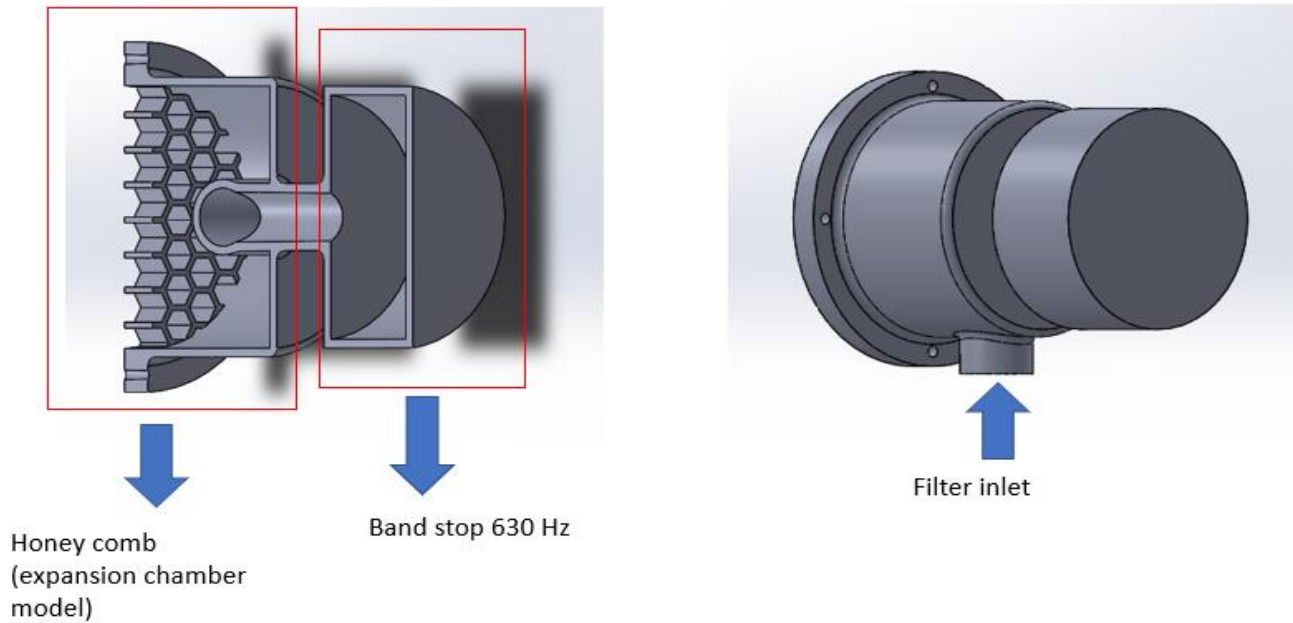
Honey comb
(expansion chamber
model)

Band stop 630 Hz

Filter inlet

Figure 42- Filter outlet: on the left section view while o the right the isometric view

To end figure.43 shows 3D model of new filters completed with screws and figure.44 gives an idea on how this filter was realized and fixed in PAT due pump. As mentioned before new design concept was realized thanks to 3D technique in PETG, this allow to have a quite close tolerances in each part of component design and fast production process.

Figure 43- 3D model of new filter concept

Figure 44- New filter concept prototype
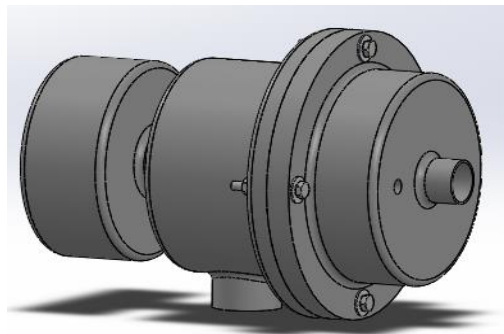
Chapter 4: Final results

4.1 PAT due new concept test results & data comparison

Here below are reported results obtained from testing of new filter concept. Figure.45 shows sound power spectrum frequency of Pat due machine in three different configurations: without filter, with the actual filter and with new concept. Those three tests were effectuated during the same day in open field environment at standard environment conditions (external temperature 20° and pressure 1 bar). Moreover, $L_w(A)$ standards were employed to evaluate overall machine noise emitted. From the graph it is possible to observe that new filter concept impacts (like the original version) in sound power spectrum in frequency range between 50-800[Hz], in addition it's worth to notice that new filter concept curve is always below the actual Pat due filter curve but both of them doesn't give consistent improvement in high frequency range.
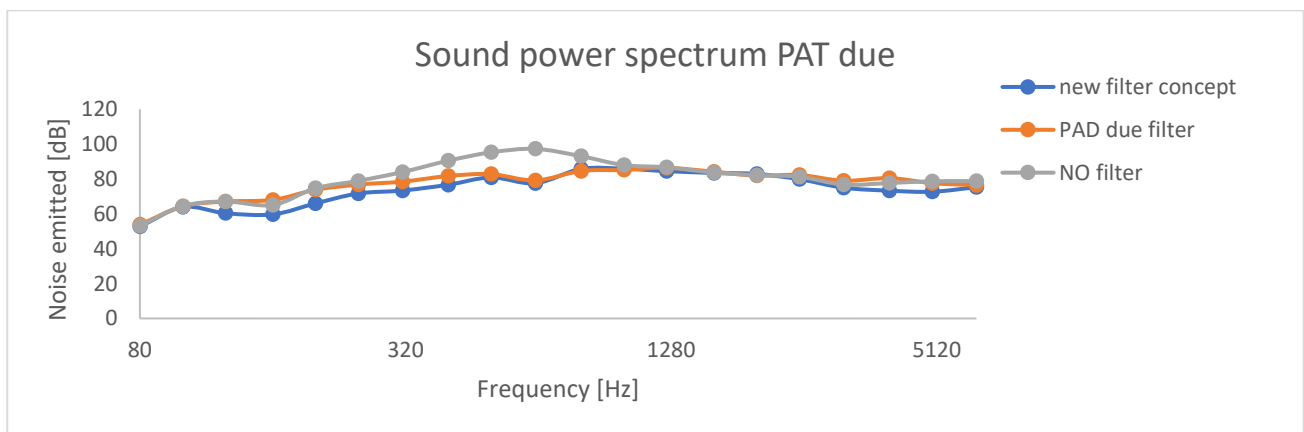

Figure 45 – Sound power spectrum frequency comparison

Figure.46 reports experimental transmission loss curves of new concept and PAT due it is evident that those filter present a pick in frequency range between 550-650 Hz and basically doesn't work in high frequency range except for new filter concept that reduces a small portion of sound near 5100 Hz frequency band. In addition is evident that new filter concept performances are always better that the previous version mostly in low frequency band, in average it improves of 5 dB the sound power spectrum frequency between 80 Hz-500 Hz.
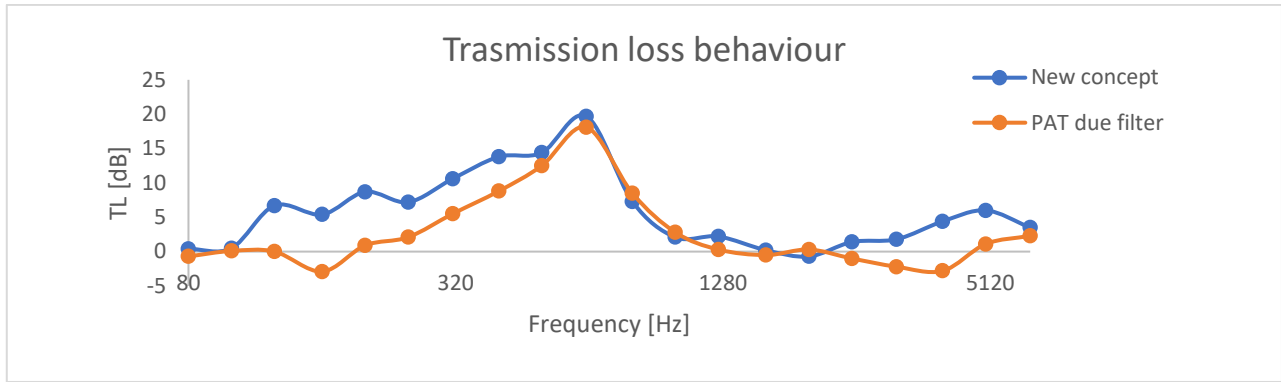
Figure 46- Transmission loss experimental results

Finally, table.17 reports overall sound power ($L_w(A)$) emitted by machine equipped with these two different filters, it is worth to observe that even if there is an average improvement in low frequency range (5dB) the overall machine noise with new acoustic device was improved by only 1.1 dB respect to the previous version and by 8.6 dB respect to no filter machine.

PAT due test	No filter	PAT due filter	New concept
$L_w(A)$ [dB]	101.5	94	92.9
Net gain in [dB]		7.5	8.6
Net improvement [dB]			1.1

Table 17- Overall sound power data comparison

4.2 Data comparison with analytical and numerical model

Figure.47 shows sound power spectrum comparison between experimental results, analytical model and Ansys model. It's possible to observe that in low frequency range both Ansys model and analytical one follow curve's trend of experimental results while in high frequency range (above 800 Hz) no one of the model gives good results, but they show high sound reduction respect the real filter model.
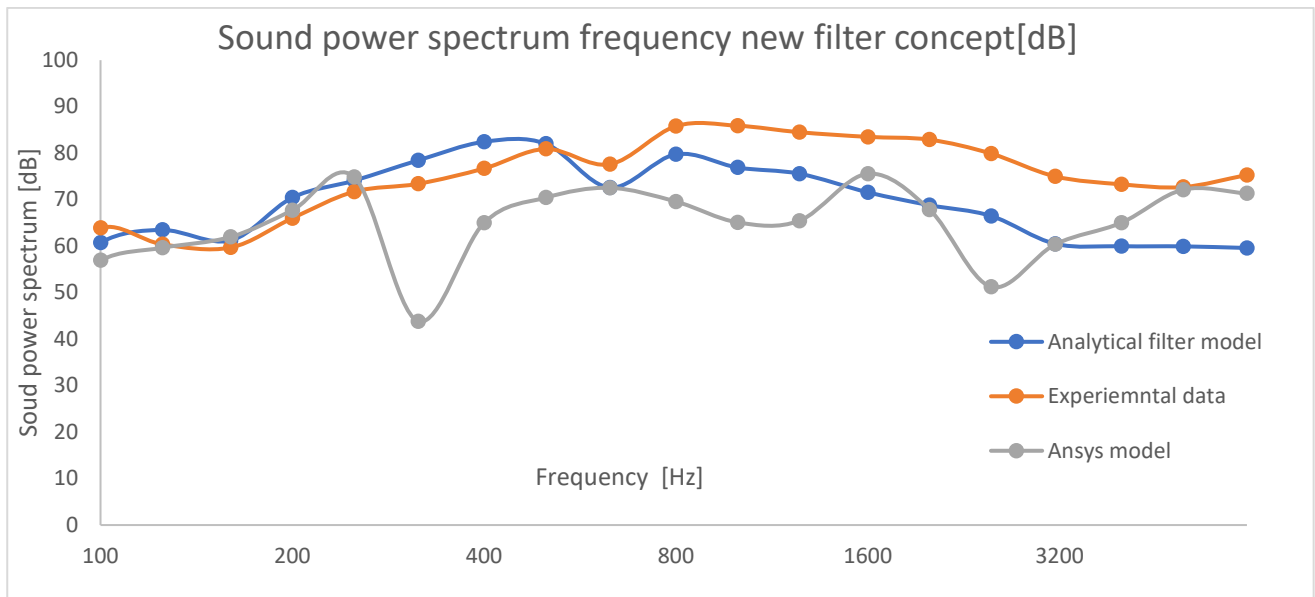
Figure 47- Sound power spectrum comparison between model and experimental results

It's worth to highlight the same data showed I previous graph in low frequency range it is easy to observe that both model in a range between [100Hz-800Hz] follow the curve's trend of experimental data. In addition, it was confirmed that analytical model is more reliable than Ansys one. Table.4 reports the sensitivity analysis that compare experimental result with ones predicted by two different models (analytical and Ansys model).
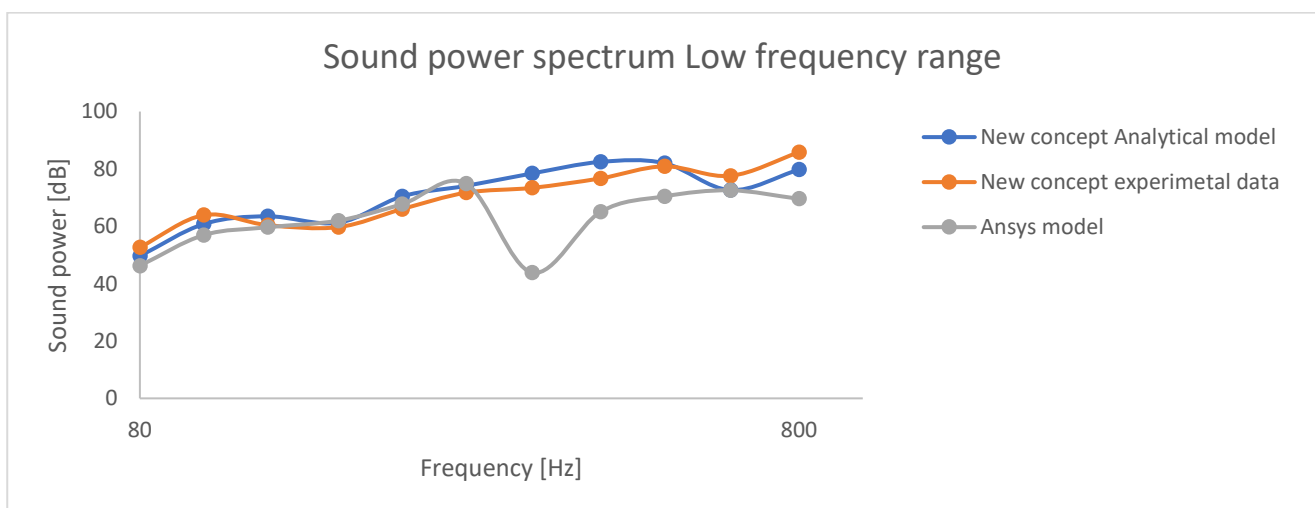

Figure 48- Sound power spectrum frequency comparison model

Table.18 depicts the sensitivity analysis of new concept device; it compares the experimental sound power spectrum frequency of new concept in all frequency range (from [100hz-6.3kHz]) whit the two theoretical one and express the difference in percentage between them. The error percentage (%error in Lw average) in sound power is evaluated by the average difference between each value of sound power emitted on each 1/3 octave frequency band (%error in Lw average) and percentage

Max .In addition, the third column shows the frequency where the maximum error between model and experiment is present.

NEW filter concept Sensitivity analysis	*%error in Lw average*	%error Max in Lw	Frequency band of max error
Analytical model	10%	21%	6.3 kHz
Ansys model	14%	40%	350 kHz

Table 18 :sensitivity analysis new concept all frequency range (100[Hz]-6.3 [kHz])

It worth to highlight also the sensitivity analysis in low frequency range (100[Hz]-800[Hz]), the same format table is reported below, it shows reliable results compared to table 4 in both models. In addition, it's evident that Ansys model is mainly affected by error at [350Hz] also in low frequency range but It is still better than previous results.

NEW filter concept Sensitivity analysis Low frequency range	%error in Lw in average for selected frequency range	%error Max in Lw	Frequency band of max error
Analytical model	5%	7%	200 Hz
Ansys model	11%	40%	350 Hz

Table 19: sensitivity analysis LOW frequency range ([100Hz]-800[Hz])

Sensitive analysis depicts that previous model are reliable mainly in low frequency range and can't describe the reality properly for frequency above 800Hz. This means that this approach can be used to proper size acoustic filter for low frequency range and have effectively sound reduction for overall machine's noise emitted. Moreover, it is evident that analytical approach is close to experimental results that in this case present an unexpected pick at (350Hz) that determine lack of accuracy.

4.3 Conclusion

Figure.49 compares PAT due sound power spectrum frequency of the new concept filter with actual one and machine not equipped with any filter. It is evident that both two consistently reduce the sound power respect to the same machine not equipped with acoustic filter till a frequency of 800 Hz. Moreover, data shows that new filter concept improve the overall noise emitted for a wide frequency range respect to the previous design filter, this behaviour is evident mostly in all frequency range except for 800 Hz and 1kHz frequencies band. This behaviour can be justified because actual filter follows the band stop model descripted in chapter 3 and works mainly near 630 Hz where there is maximum noise reduction, while new filter

concept was designed to works for widely frequency range because it is thought as a combination of two different acoustic filter (band stop model and expansion chamber).
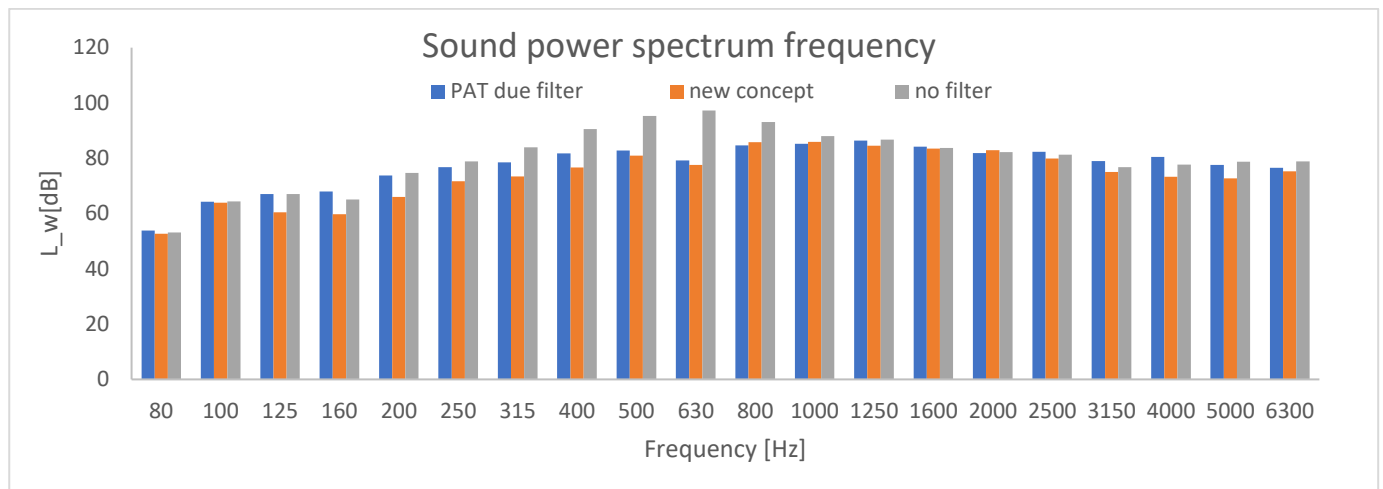

Figure 49- Sound power spectrum between three machines set up

Figure.50 shows the sound power spectrum frequency comparison between new concept and no filter equipped machine, it depicts that new filter design works mainly in low frequency range where is present a consistent reduction of sound power emitted while in frequency band above 800Hz there is still an improvement in acoustic performance but not so evident gain event if the previous model predicted different results in high frequency range.
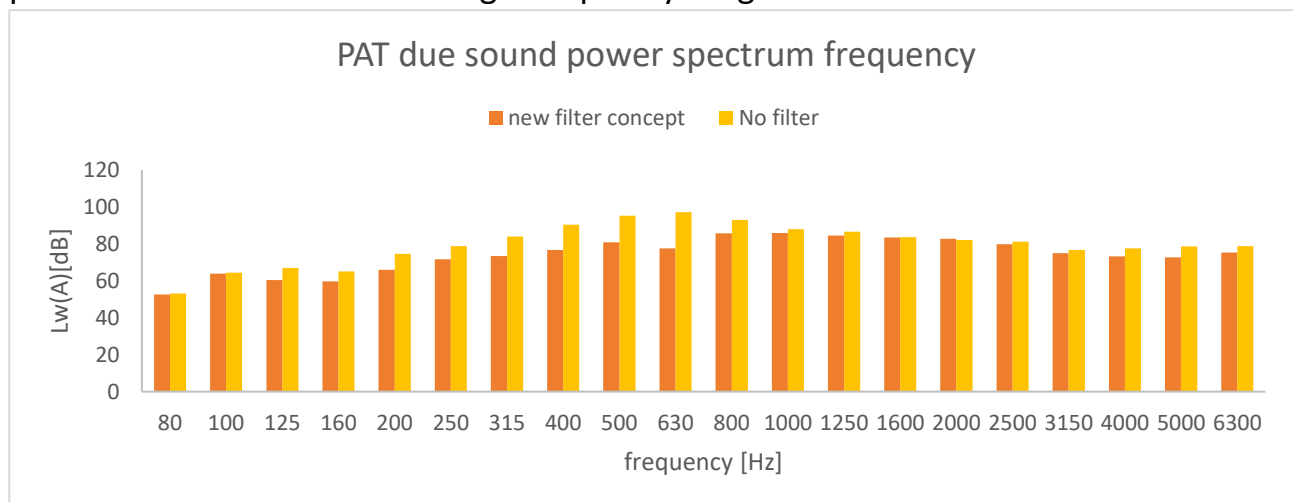
Figure 50- Data comparison new concept and no filter

Finally, figure.51 reports the comparison between new concept and the previous designed one, it shows that in average new designed one is better in all frequency range respect to the actual one except for few frequency band, so even if the overall gain respect to the actual one is 1.1 dB , it improved the machine acoustic.
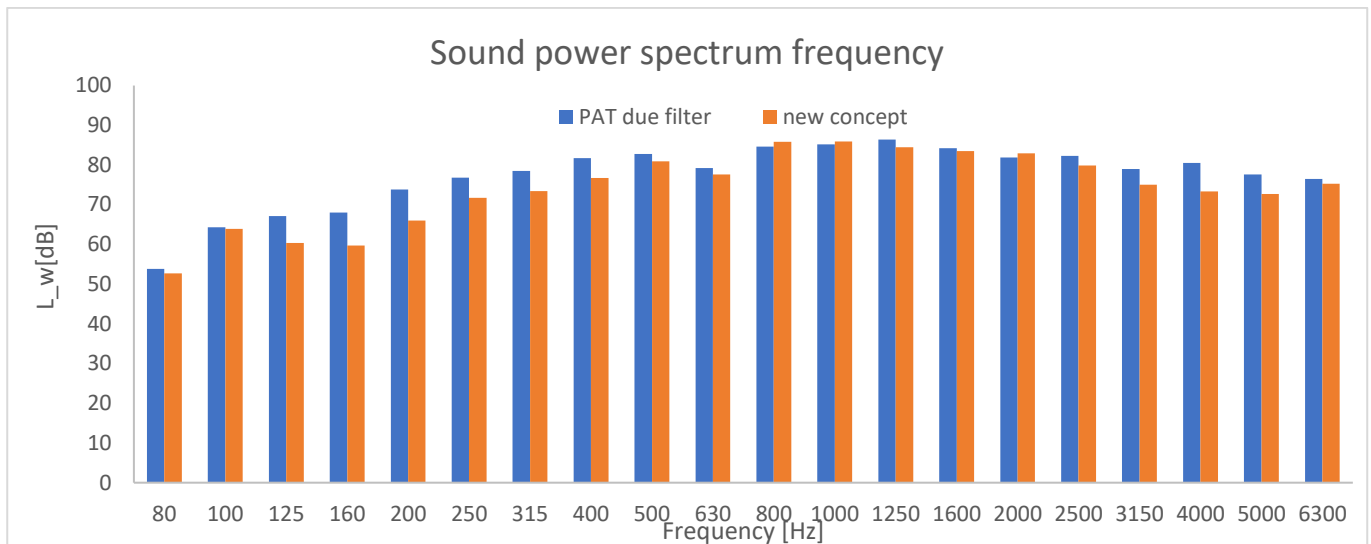
Figure 51- Sound power spectrum frequency comparison between new concept and actual design

To conclude, the approach presented in this paper results reliable to design an acoustic filter in low frequency range and shows that the overall machine noise can be improved by looking to other noise sources. Moreover, it's worth to highlight that air pulsation travels with low frequency and this explain why new filter concept don't reflect back any waves that travel with frequencies higher than 800[Hz]. In addition, sound power spectrum frequency highlight that the most relevant frequencies that affects the machine noise are the high frequency range (above [1kHz]) and new filter concept doesn't consistently affect the acoustic performance in that range so this bring to think that this issue could be solved in different way.

Chapter 5: Further improvement

5.1 Pressure drop in filter

Design procedure to realize new filter concept was meant only to reduce overall sound emitted by the machine firstly considering the air pulsation that comes from external condition. New design concept doesn't consider the pressure drop between external air condition and internal compression stage. Experimental results showed that are present high losses due to pressure drop between new filter concept and the actual Pat due filter, this slightly penalize the machine performances (FAD). Table.20 shows how the new filter concept penalizes FAD performance even thought there it improves acoustic overall acoustic performance. It is evident that new filter decreased inlet effective p_1 this lowered consistently decreased the free air delivery by 130 l/min.

	No filter	PAT due filter	New concept
FAD [l/min]	582	436	303
Pressure drop [bar]	0	0.22	0.45
Efficiency	100%	75%	52%
p_1 **[bar]**	1	0.78	0.55

Table 20 FAD comparison between filters

This result brings to conclude that it is not possible design new filter considering only the positive effects that it gives to the overall sound power emitted but should be considered also the pressure drop that it eventually creates. In order to estimate pressure drop due to filter element it is possible to consider different model that describes this phenomena that derives from Bernulli law. Equation.39 is one of possible method to depicts and evaluate pressure drop down the filters, it consider speed and fluid density and geometry parameters of the filter that is modelled like a duct, moreover that model takes into account fluid frictions thanks to two adimensional factors equation 5.2 and 5.3. It is relevant that what mainly affects pressure drop in that component is the equivalent length L that is affected by all impedances that fluid pass from inlet to outlet table.21 shows how equivalent length change when fluid hit an obstacle during its flow. All value present in table below are multiplication factor that increase the equivalent length L as fuction of obstacles.

$$dp = f \frac{L}{D} \frac{u^2 \rho}{2}$$

Equation 39- Experimental pressure drop law

$$f[fanning\ friction\ factor] = \frac{0.0791}{R_e^{0.25}}$$

Equation 40- Fanning friction factor

$$R_e[Reynolds\ number] = \frac{\rho u L}{\mu}$$

Equation 41- Reynold number

Where:

- dp $pressure\ drop$ $[Pa]$
- $f[]$ $is\ the\ finning\ faction\ that\ represnt\ a\ dimension$
- $L[m]$ $is\ the\ equivalent\ pipe\ lenght$
- $D\ [m] is\ the\ diameter\ of\ the\ pipe$
- $\rho[Kg/m^3] is\ the\ air\ dencity\ in\ standard\ condition$

- *μ dynamic viscosity of air*
- *u [m/s] fluid avarage speed*

	Equivalent length coefficient L				
	Pipe diameters in D [mm]				
Impedance type	25	40	50	80	100
 Figure 52-Elbow junction R=D	0.3	0.5	0.6	1	1.5
 Figure 53- Elbow junction R=2D	0.15	0.25	0.3	0.5	0.8
 Figure 54-"Ti" junction	2	3	4	7	10
 Figure 55-Reduction pipe	0.5	0.7	1	2	2.5

Table 21-Equivalent length pipe value

To conclude next step to improve actual filter design is to consider losses due to obstacle that actual filter has to overcame before flowing into first compression stage. New filter concept has two relevant impedances that obstacles fluid first Ti junction at the inlet and second the honey-comb grid, those two massively affects the equivalent length of the component that turn to increase the pressure drop.

5.2 Vibrations in high frequency range

Sound power spectrum frequency shows that high frequencies are the most relevant in the all frequency range and the inlet filter doesn't filter those frequencies so this bring to think that in order to further decrease machine noise, vibration needs to be considered. Vibration test were performed together with acoustic test using triaxial accelerometers and they showed high acceleration picks above 1k[Hz] frequency so it will be interesting to investigate is those picks are related with sound power spectrum and look for solutions to solve this issue. Here below are

reported results were collected during vibrations test. Accelerometers were placed in 5 different position for each of them accelerations will be collected for each axis. Again, the same signal analyser used for noise test was employed to take this experimental data. Reference system that characterize the accelerometers is defined as follow:

- *z axis is the one ortogonal to the pump shaft*
- *x axis is alliened with shaft axel*
- *y axis is* orthogonal to the other two and aligned to tank axis

Figure 56- Experimental set up vibration test point 1
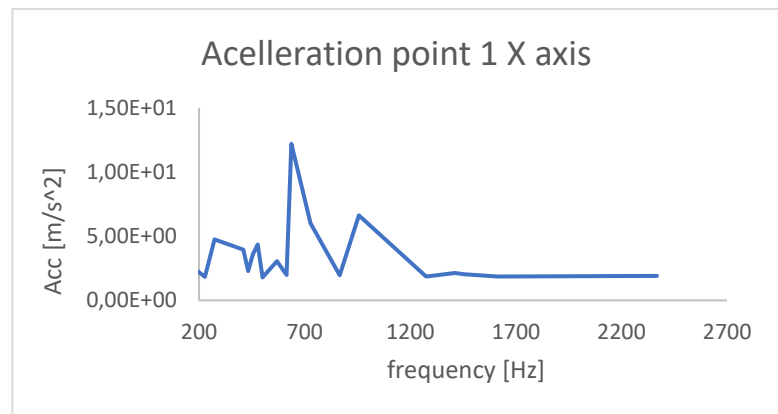
Figure 57- Accelerometer data pint 1 X axis
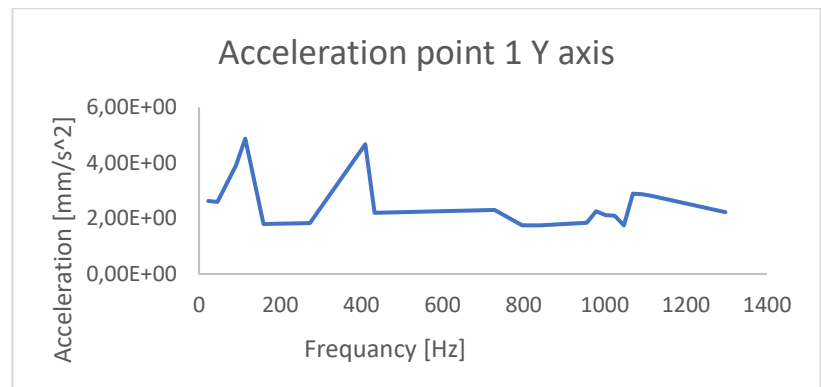
Figure 58- Accelerometer data point 1 Y axis
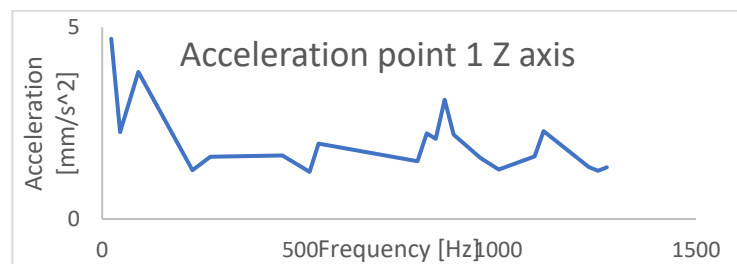
Figure 59- Accelerometer data point 1 Z axis

Figure 61- Accelerometer data point 2 X axis
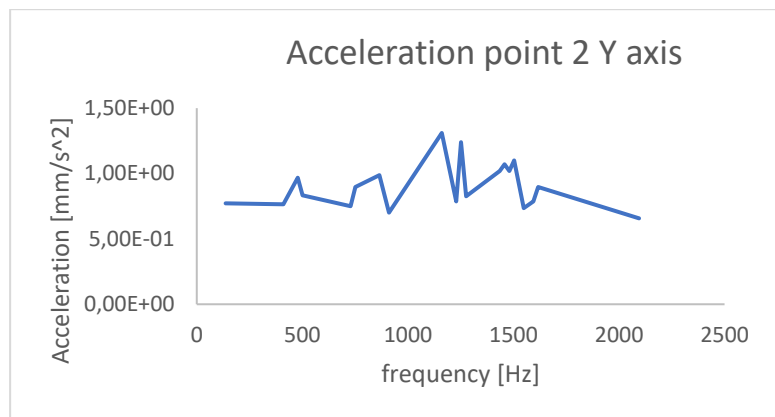
Figure 62- Accelerometer data point 2 Y axis

Figure 60- Experimental set up vibration test point 2
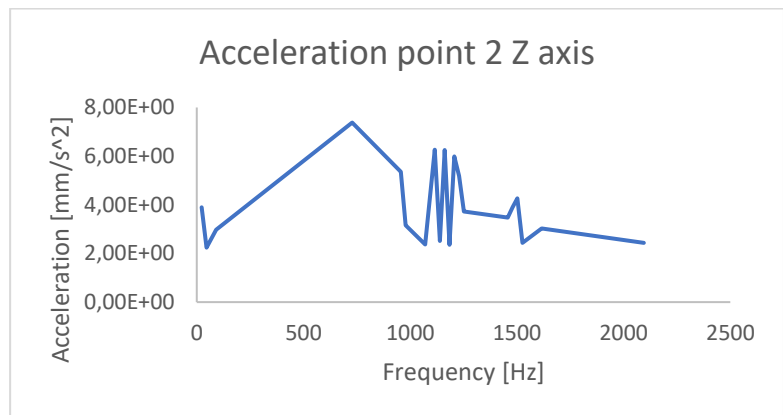
Figure 63- Accelerometer data point 3 Z axis

Figure 65- Accelerometer data x axis point 3
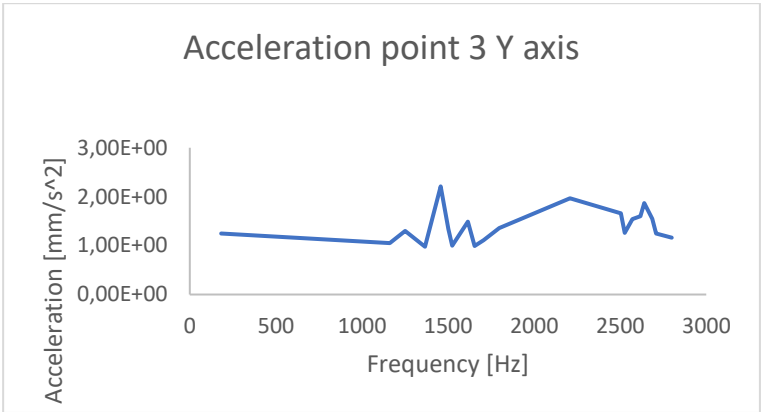
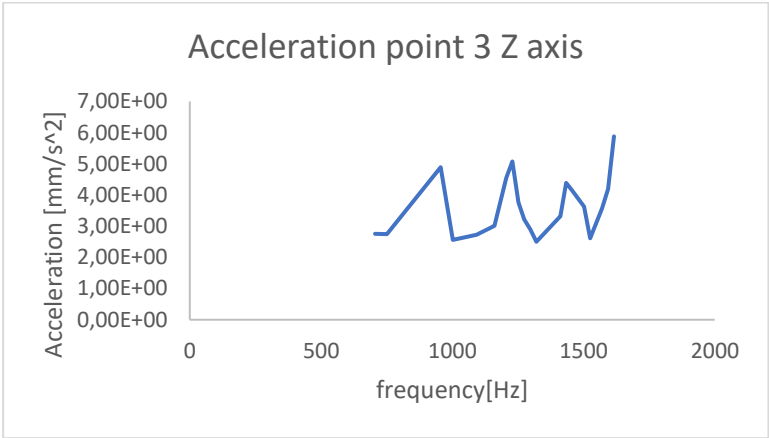Figure 66- Accelerometer data Y axis point 3

Figure 67- Accelerometer data Z axis point 3
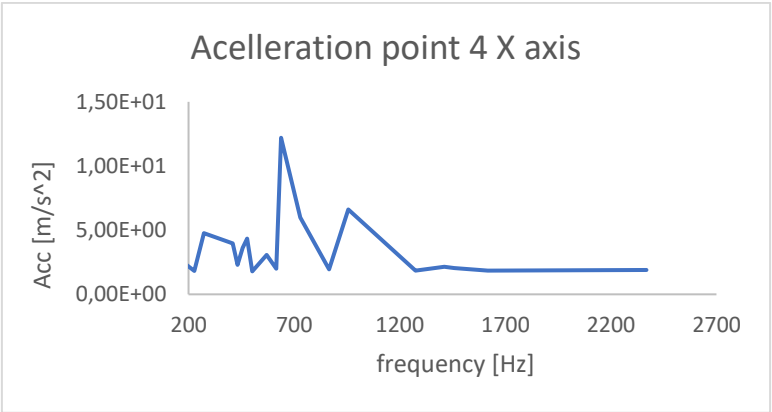

Figure 64- Experimental set up vibration test point 3

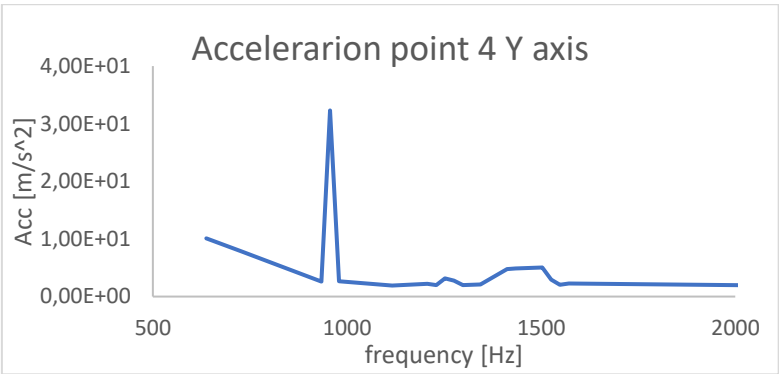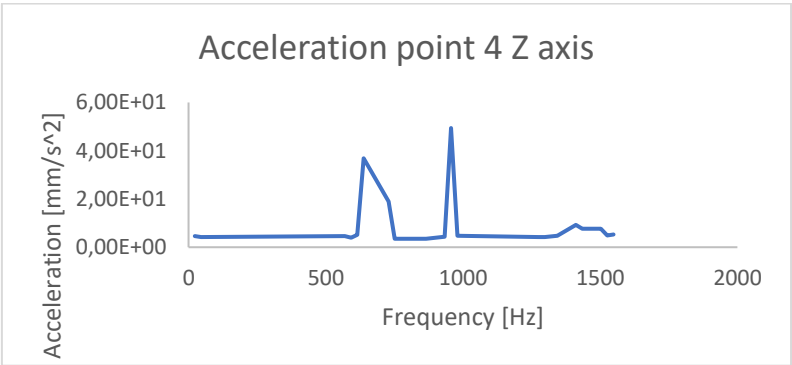Figure 69- Acceleration data point 4 X axis

Figure 70- Acceleration data point 4 Y axis

Figure 71- Acceleration data point 4 Z axis

Figure 68- Experimental set up vibration test point 4
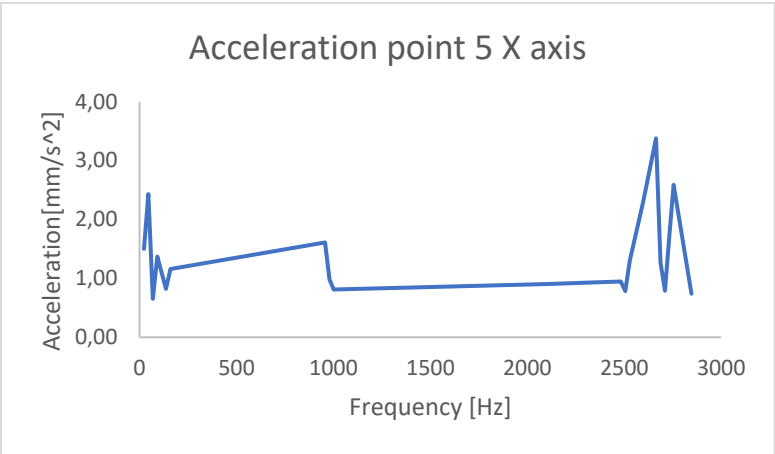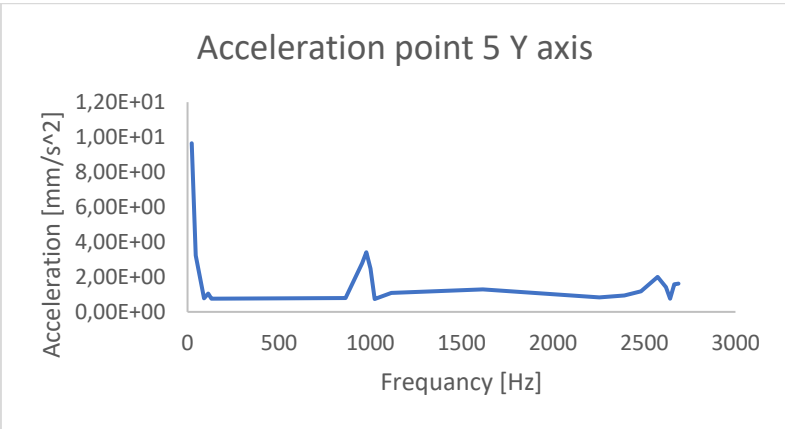
Figure 73 -Acceleration data point 5 X axis

Figure 74- Acceleration data point 5 Y axis

Figure 72- Experimental set up vibration test point 5

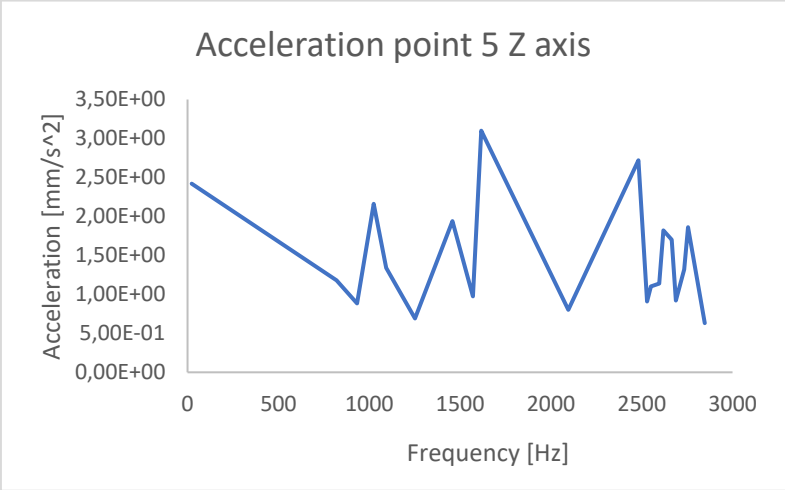*Figure 75- Acceleration data point 5 Z axis*

References

[1]   W. Soedel, *Sound and vibration of Positive Dispacement Compressors*. 2007.

[2]   C. H. Hansen, "1 fundamentals of acoustics," 1994.

[3]   D. A. Russell, "Acoustic High-Pass , Low-Pass , and Band-Stop Filters," no. April, 2018.

[4]   R. Galgalikar, "DESIGN AUTOMATION AND OPTIMIZATION OF HONEYCOMB STRUCTURES FOR MAXIMUM SOUND," 2012.

[5]   J. Jung, S. Hong, J. Song, and H. Kwon, "A Study on Transmission Loss Characteristics of Honeycomb Panel for Offshore Structures," no. February, pp. 172–176, 2015.
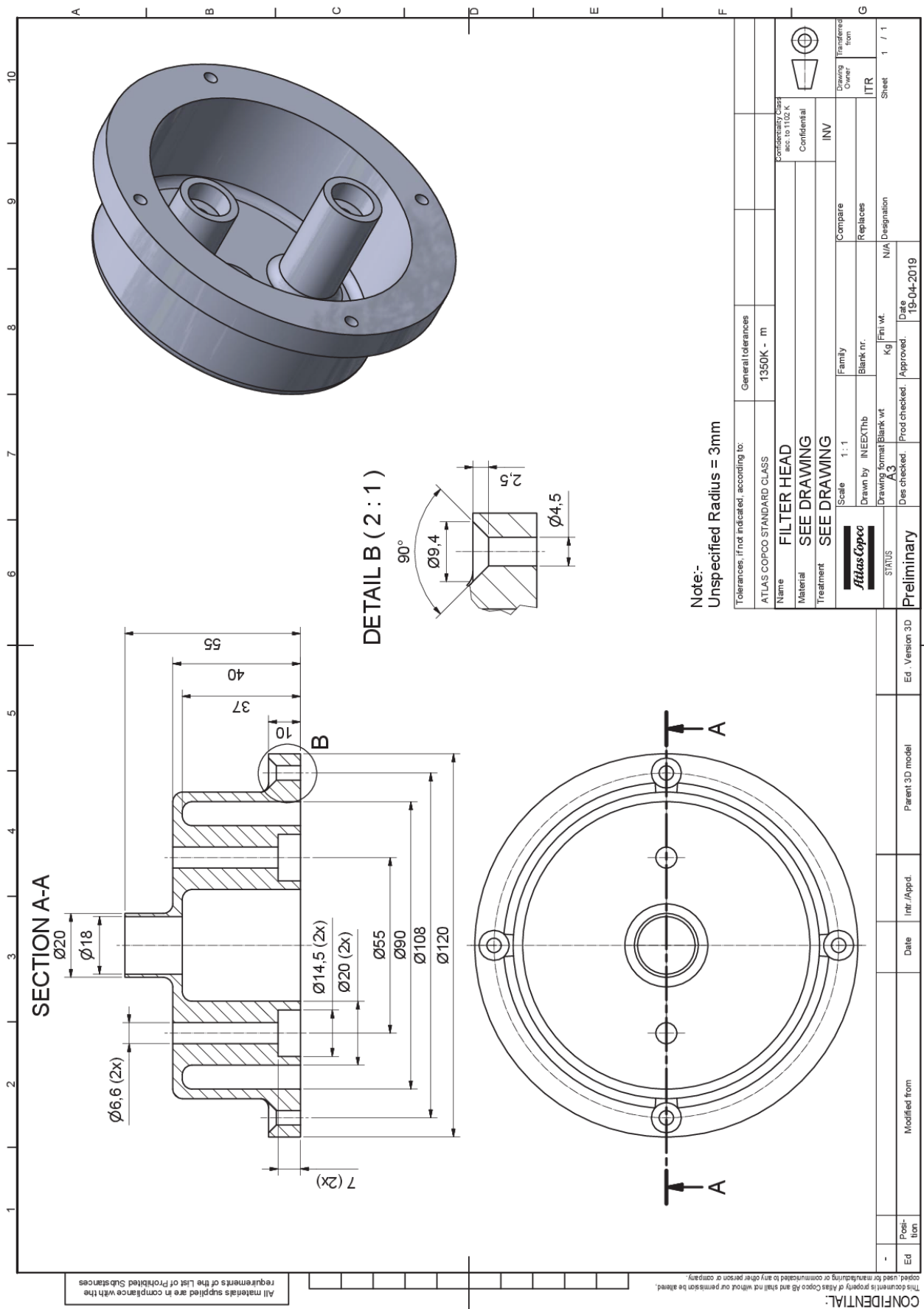
Appendix- Technical drawings

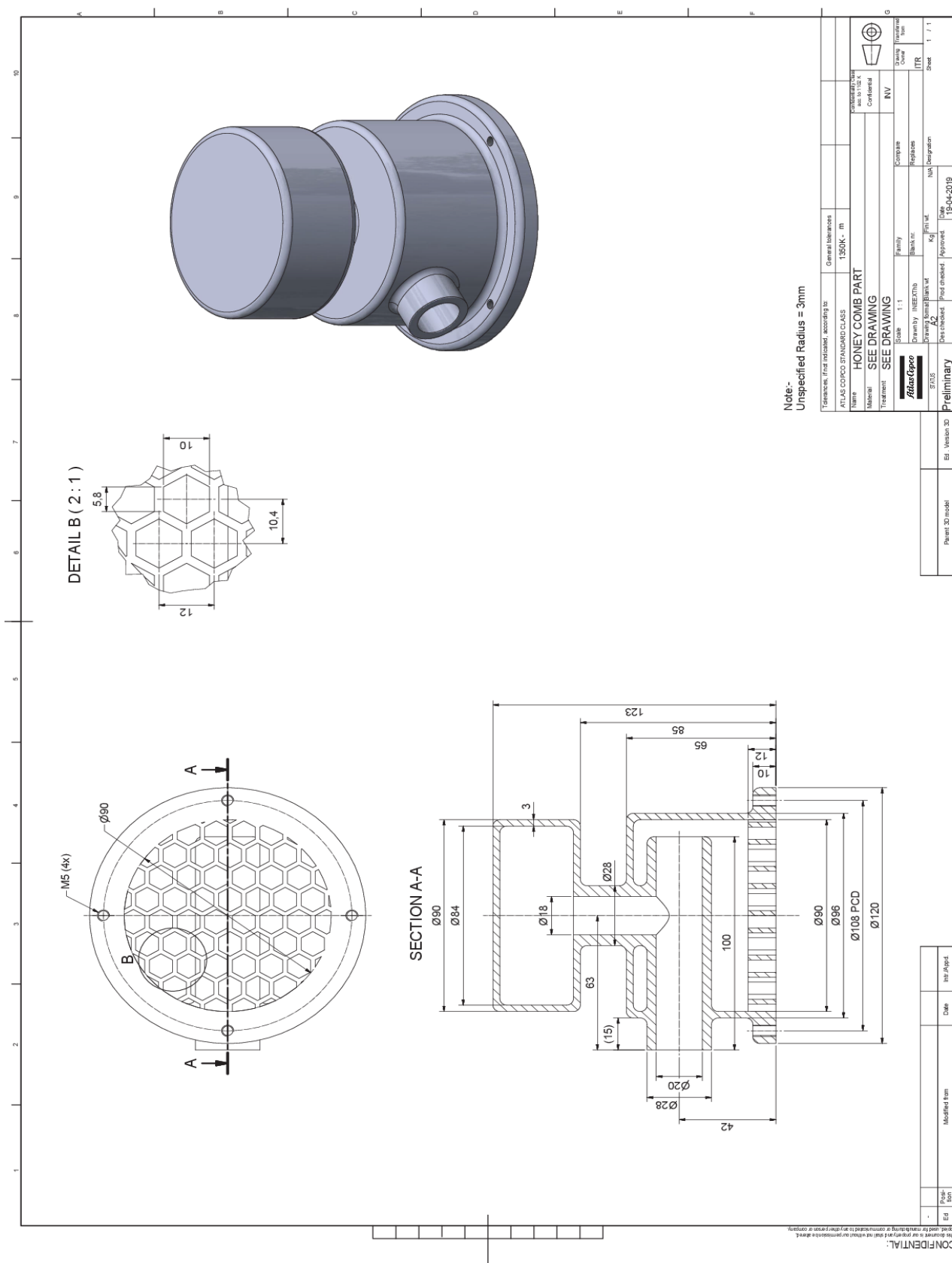*Figure 76- New concept filter assembly technical drawing*

Figure 77- New concept filter outlet technical drawing
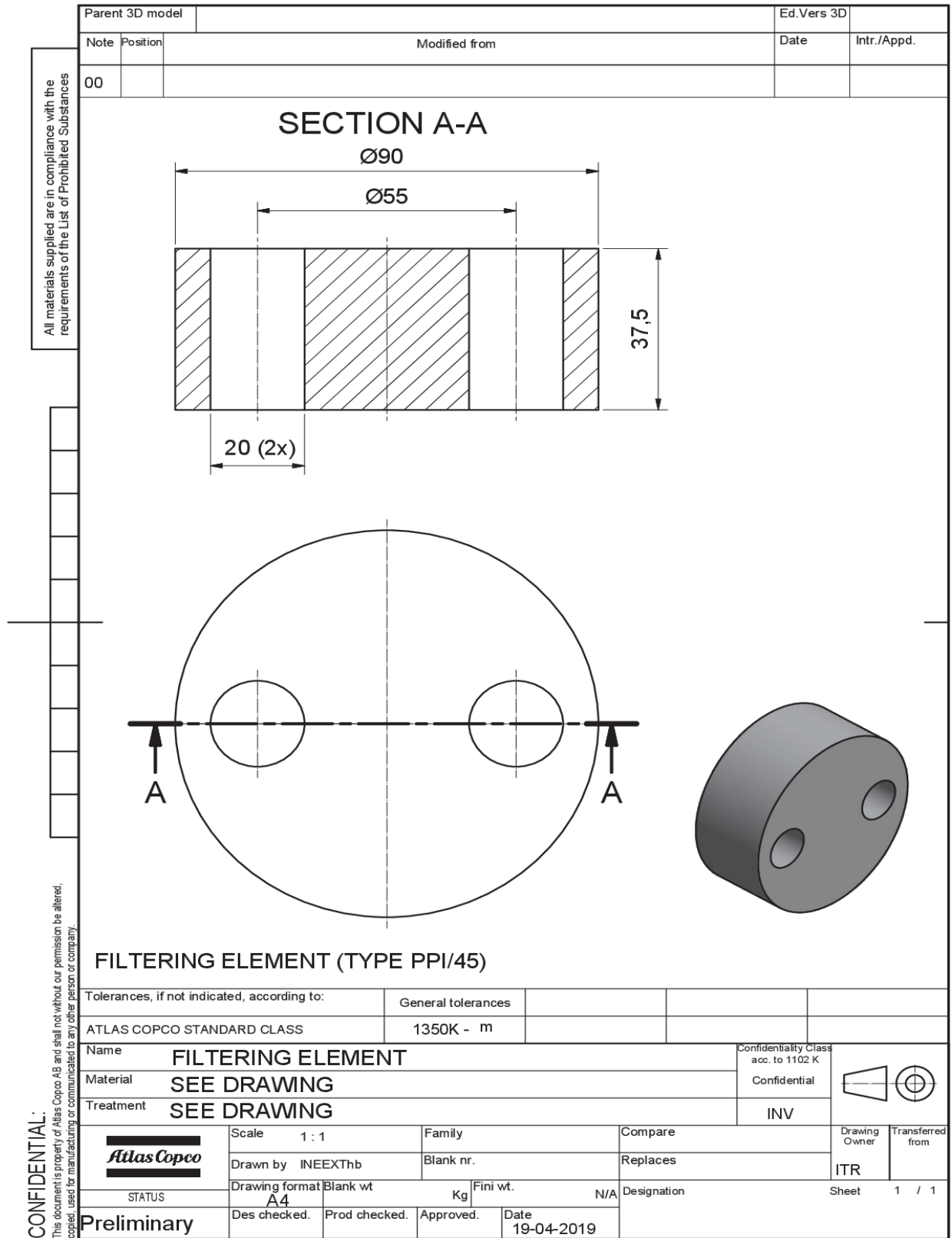
Figure 78- New concept filter inlet technical drawing

Figure 79- New concept foam material technical drawing